

Calculation of the α -particle ground state within the hyperspherical harmonic basis

M. Viviani,¹ A. Kievsky,¹ and S. Rosati^{1,2}¹*Istituto Nazionale di Fisica Nucleare, Via Buonarroti 2, I-56100 Pisa, Italy*²*Dipartimento di Fisica, Università di Pisa, Via Buonarroti 2, I-56100 Pisa, Italy*

(Received 6 August 2004; published 25 February 2005)

The problem of calculating the four-nucleon bound state properties for the case of realistic two- and three-body nuclear potentials is studied using the hyperspherical harmonic (HH) approach. A careful analysis of the convergence of different classes of HH functions has been performed. A restricted basis is chosen to allow for accurate estimates of the binding energy and other properties of the ${}^4\text{He}$ ground state. Results for various modern two-nucleon and two- plus three-nucleon interactions are presented. The origin of the isospin $T = 1$ and $T = 2$ admixtures in the ${}^4\text{He}$ ground state is discussed in detail. The ${}^4\text{He}$ asymptotic normalization constants for separation in $2 + 2$ and $1 + 3$ clusters are also computed.

DOI: 10.1103/PhysRevC.71.024006

PACS number(s): 21.45.+v, 27.10.+h, 21.30.-x, 21.10.Dr

I. INTRODUCTION

Rapid progress has been made during the last few years in the quantitative study of the $A = 4$ nuclear systems. Ever-increasing computer power, development of novel numerical methods, and significant refinements of well-established techniques have allowed the solution of the four-nucleon bound state problem with a control of the numerical error at the level of 10–20 keV [the experimental α -particle binding energy (BE) being 28.30 MeV], at least for Hamiltonians including only nucleon-nucleon (NN) interaction models [1]. In the latter work, the BE and other properties of the α particle were studied with the AV8' [2] NN interaction, and the different techniques produced results in very close agreement with each other (at the level of less than 1%).

In Refs. [3,4], realistic potential models have been used to describe the α -particle bound state. Those potential models consist of the sum of a modern NN interaction plus a three-nucleon ($3N$) interaction. A modern NN interaction has the property of describing the NN database with a χ^2 per datum close to 1. Examples are the Argonne V18 (AV18) potential [5], the Nijmegen potentials [6], the CD-Bonn potential [7,8], and the recently proposed potential, nonlocal in r space, developed by Doleschall and Colleagues [9,10]. This last potential has the remarkable property of reproducing simultaneously the NN bound and scattering data and the $3N$ binding energies (although, it predicts a too-low rms radius for the α particle [11] and cannot reproduce the spectrum of ${}^6\text{Li}$ [12]). As is well known, the other models (AV18, Nijmegen, and CD-Bonn) underbind the $3N$ system. Usually a $3N$ interaction is included in the Hamiltonian when these potentials are considered. The strength of the $3N$ interaction is properly tuned to reproduce the ${}^3\text{H}$ binding energy and this strength depends on the chosen NN potential. Examples of $3N$ interactions are the Urbana IX (UIX) [2], Tucson-Melbourne (TM) [13], and Brazil [14] potentials. From Ref. [3] we observe that all the $NN+3N$ potential models that reproduce the deuteron and the $3N$ binding energies slightly overbind the α particle. We further observe that the results obtained for the AV18+UIX potential model using different techniques (see Refs. [3,4]), though close to each other, are not in complete agreement. Clearly

a clarification of these points would be welcome. Moreover, in recent years there has been a rapid progress in developing new models of the NN interaction based on the application of the chiral perturbation theory (CPT) [15–18]. In particular, the NN potential of Ref. [18] reproduces the two-nucleon data with a χ^2 per datum close to 1, as the other NN potentials mentioned above. Moreover, there has been also some progress in developing $3N$ interaction models in a consistent and systematic way in the framework of the CPT [19]. From these studies one can hope to have a better understanding of the form of the NN and $3N$ interactions (the four-nucleon force is expected to be very small). All these potential models have to be studied in detail in the $A = 3$ and $A = 4$ systems. It is therefore very important to have powerful techniques for solving four-nucleon problems.

The methods devised to tackle the problem of the solution of the nonrelativistic Schrödinger equation

$$H\Psi(1, 2, 3, 4) = E\Psi(1, 2, 3, 4), \quad (1)$$

where H is the four-body nuclear Hamiltonian, are very different. In the Faddeev–Yakubovsky (FY) approach [3,11,20–24], Eq. (1) is transformed to a set of coupled equations for the FY amplitudes, which are then solved directly (in momentum or coordinate space) after a partial wave expansion. In the green function Monte Carlo (GFMC) method [4,25] one computes $\exp(-\tau H)\Phi(1, 2, 3, 4)$, where $\Phi(1, 2, 3, 4)$ is a trial wave function (WF), using a stochastic procedure to obtain, in the limit of large τ , the exact ground state WF Ψ . These two techniques have also been applied to the case where the nuclear Hamiltonians includes a $3N$ interaction. The stochastic variational method (SVM) [26,27] and the coupled rearrangement channel Gaussian-basis method (CRCG) [28,29] provide a variational solution of Eq. (1) by expanding the (radial part of the) WF in Gaussians. The two techniques differ in the way they determine the nonlinear coefficients of the expansion: in the SVM random choices are used to select the optimum set, whereas in the CRCG technique the nonlinear coefficients are chosen in geometrical progression in such a way that only a few of them have to be varied. Very recently two other new techniques have been proposed.

In the no-core shell model (NCSM) method [12,30–32] the calculations are performed using a (translational-invariant) harmonic-oscillator (HO) finite basis P and introducing an effective P -dependent Hamiltonian H_P to replace H in Eq. (1). The operator H_P is constructed so that the solution of the equation $H_P\Psi(P) = E_P\Psi(P)$ provides eigenvalues that quickly converge to the exact ones as P is enlarged. The effective interaction hyperspherical harmonic (EIHH) method [33,34] is based on a similar idea, but the finite basis P is constructed in terms of the hyperspherical harmonic (HH) functions.

In the present work we address the problem of calculating the α -particle properties, using a nuclear Hamiltonian containing modern two- and three-nucleon interactions, by expanding the WF in terms of the HH functions. Our intention is to obtain converged binding energies at the level of 20–30 keV. The motivation is twofold. First we would like to reduce the theoretical error in the determination of the α -particle bound state properties. Second, the HH techniques can also be extended to treating four nucleons scattering states, as has been possible for the $A = 3$ system [35] using a similar technique. This program is currently underway and a preliminary report has been already published [36]. The richness of phenomena in the four-nucleon scattering and reactions will be an ideal laboratory for studying and testing newer models of the nuclear interaction. At present, the theoretical calculations based on the current NN and $3N$ interactions show large discrepancies with some four-nucleon scattering data [23,37–39].

In an earlier work [40], the authors determined the solution of Eq. (1) variationally by expanding the WF in a basis of correlated hyperspherical harmonic (CHH) WFs. The space part of such a basis consisted of products of correlation factors F and HH functions. The correlation factors F were chosen so as to take into account the strong correlations induced by the NN potential, especially at short interparticle distances. The introduction of such factors substantially improved the convergence of the expansion. This made it possible to obtain reasonable estimates for the ground-state energy of the α particle and some selected observables in n - ^3H and p - ^3He elastic scattering using a rather limited basis set [38,40,41]. However, because of the complexity of F , the spatial integrations were performed by using quasirandom number techniques. The precision of the required matrix elements was therefore limited, and the inclusion of a greater number of states was problematic.

When the four-nucleon WF is expanded in terms of the uncorrelated HH basis (i.e., setting $F = 1$) most of the integrations can be performed analytically, and the remaining low-dimensional integrals can be evaluated by means of efficient quadrature methods. However, because of the particular structure of the NN potential, which is state dependent and strongly repulsive at short distances, a very large number of basis elements are required. For that reason, the application of the HH technique to studying the $A = 4$ nuclear system has encountered serious convergence problems. Few four-body HH calculations have been attempted so far for realistic interactions [42–44]. Even for central or super-soft-core potentials the problem of the slow convergence of the HH

expansion has not been completely overcome [42,44,45]. The reason for these difficulties is related to the slow convergence of the basis with respect to the grand angular quantum number K and to the large number of HH states with a given K . For example, for an accurate description of the α -particle ground state, antisymmetric spin-isospin-HH states up to $K = 60$ have to be included. However, the number of such states already for $K = 20$ is greater than 1000 and it increases very rapidly with K . It is therefore clear that a brute force application of the method is not possible even with sophisticated computational facilities.

The approach analyzed in the past was to select a suitable subset of states [46–48]. In those articles it resulted quite clearly that the quantum number K is not the unique parameter important for studying the convergence of the basis. Let us recall that a four-body HH function is specified by three orbital angular momentum quantum numbers, ℓ_1, ℓ_2, ℓ_3 , and two additional quantum numbers, n_2 and n_3 (which are nonnegative integers), related to the radial excitation of the system. The grand angular quantum number is defined to be $K = \ell_1 + \ell_2 + \ell_3 + 2(n_2 + n_3)$. Note that $\mathcal{L} = \ell_1 + \ell_2 + \ell_3$ and K are even (odd) numbers for positive (negative) parity states. In Ref. [46], the basis was restricted to including HH states with a few choices of ℓ_1, ℓ_2, ℓ_3 values and large values of n_2 and n_3 . The calculations performed [42,43] were, however, limited by the computer power available at that time. In this article, it is shown that HH states having $\mathcal{L} \equiv \ell_1 + \ell_2 + \ell_3 \leq 6$ are sufficient to obtain a four-digit convergence. However, the number of HH states with $\mathcal{L} \leq 6$ is still huge and additional criteria for selecting a reduced basis have to be specified.

It is possible to organize the HH states in terms of the number of particles correlated. For example, there is a class of basis elements that depends only on the coordinate of two particles, the so-called potential basis (PB) [48]. Such a basis therefore takes the two-body correlations into account. However, even in the case of simple model interactions, the BE's B obtained by restricting the expansion basis to the PB were found to be rather far from the exact values. For example, for the Malfliet-Tjon V (MT-V) central potential [49], B calculated with the PB is approximately 1 MeV smaller than the exact value. For a realistic potential the situation is noticeably worse. However, it is clear that the procedure of classifying the HH states in terms of the number of correlated particles can be useful for distinguishing the importance of the various expansion terms.

In the present article the application of the HH expansion basis is developed by taking advantage of both strategies discussed above. Namely, HH states of low values of ℓ_1, ℓ_2, ℓ_3 are included first. Among them, those correlating only a particle pair are included first, and then those correlating three particles are added, and so on. In practice, the HH states are first divided into classes depending on the value of \mathcal{L} and n_2, n_3 . Let us denote with $\mathcal{M}_i(K_i)$ the number of states belonging to a class i with $K \leq K_i$. Such a number of states rapidly increases with K_i , in general $\mathcal{M}_i(K_i) \approx M_i \times (K_i)^r$ for large K_i , where M_i are a set of numbers and $r = 1$ or 2 . The first and most important classes should contain only a small subset of HH states (“small” classes), namely their M_i should be small, let us say $M_i \approx 1$. It is then relatively easy to include HH states

of large K belonging to these classes. The classes containing successively larger numbers of states ($M_i \gg 1$) should be chosen possibly so as to contribute lesser and lesser to the expansion in such a way that the corresponding expansion can be truncated to small values of K . A careful analysis of the convergence properties of the various HH components has allowed for an optimal choice of the classes so that accurate calculations of the α -particle properties could be achieved.

An important aspect of a successful application of the HH method is related to the computation of the coefficients for the transformation of a HH function corresponding to a generic permutation of the four particles in terms of those constructed for a given permutation. Various approaches have been devised to deal with this problem [43,50–55]. The usefulness of these coefficients is twofold. First, it is easy to identify the linearly dependent states and to avoid their inclusion in the expansion basis. The removal of these “spurious” states, which disappear after a proper antisymmetrization of the basis, is very useful as the number of linear independent states is noticeably smaller than the full degeneracy of the basis. Second, the matrix elements of a local two-body (three-body) potential energy operator are easily reduced to one-dimensional (three-dimensional) integrations, which can also be performed beforehand and stored on computer disks. The matrix elements of nonlocal operators can also be reduced to low-dimensional integrals. The kinetic energy operator is easily obtained analytically.

The study presented in this article is the extension of the application of the HH expansion to the three-nucleon system performed in Ref. [56]. The natural continuation would be related to the application of the HH technique to heavier systems. In particular, we can point out that for $A > 4$ the calculation of the multidimensional integrals related to the matrix elements of a local NN ($3N$) interaction can also be reduced to a one-dimensional (three-dimensional) integration. The only difficulty in extending the method to heavier systems is the choice of a suitable and optimized subset of HH functions. We hope that the criteria used here to select an optimal subset of the basis could also be applied for systems with $A > 4$. Alternatively, one could try to integrate the present study with the effective interaction formalism [33,34].

This article is organized as follows. In the next section, a brief description of the properties of the HH functions is reported. In Sec. III, the choice of the basis is presented. The results obtained for the BE and other properties of the α particle are presented in Sec. IV. Finally, the last section is devoted to the conclusions and the perspectives of the present approach.

II. THE HH EXPANSION

For four equal mass particles, a suitable choice of the Jacobi vectors is as follows:

$$\begin{aligned}\xi_{1p} &= \sqrt{\frac{3}{2}} \left(\mathbf{r}_m - \frac{\mathbf{r}_i + \mathbf{r}_j + \mathbf{r}_k}{3} \right), \\ \xi_{2p} &= \sqrt{\frac{4}{3}} \left(\mathbf{r}_k - \frac{\mathbf{r}_i + \mathbf{r}_j}{2} \right), \\ \xi_{3p} &= \mathbf{r}_j - \mathbf{r}_i,\end{aligned}\quad (2)$$

where p specifies a given permutation corresponding to the order i, j, k , and m of the particles. By definition, the permutation $p = 1$ is chosen to correspond to the order 1, 2, 3, and 4.

For a given choice of the Jacobi vectors, the hyperspherical coordinates are given by the hyperradius ρ , defined by the following:

$$\rho = \sqrt{\widehat{\xi}_{1p}^2 + \widehat{\xi}_{2p}^2 + \widehat{\xi}_{3p}^2} \quad (\text{independent on } p), \quad (3)$$

and by a set of variables that in the Zernike and Brinkman [48,57] representation are the polar angles $\widehat{\xi}_{ip} \equiv (\theta_{ip}, \phi_{ip})$ of each Jacobi vector, and the two additional “hyperspherical” angles φ_{2p} and φ_{3p} defined as follows:

$$\begin{aligned}\cos \varphi_{2p} &= \frac{\widehat{\xi}_{2p}}{\sqrt{\widehat{\xi}_{1p}^2 + \widehat{\xi}_{2p}^2}}, \\ \cos \varphi_{3p} &= \frac{\widehat{\xi}_{3p}}{\sqrt{\widehat{\xi}_{1p}^2 + \widehat{\xi}_{2p}^2 + \widehat{\xi}_{3p}^2}} = \frac{\widehat{\xi}_{3p}}{\rho},\end{aligned}\quad (4)$$

where $\widehat{\xi}_{jp}$ is the magnitude of the Jacobi vector $\widehat{\xi}_{jp}$. The set of the variables $\widehat{\xi}_{1p}, \widehat{\xi}_{2p}, \widehat{\xi}_{3p}, \varphi_{2p}, \varphi_{3p}$ is denoted hereafter as Ω_p . To simplify the notation for $p = 1$, the subscript 1 will sometimes be omitted. The expression of a generic HH function is as follows:

$$\begin{aligned}\mathcal{Y}_{\ell_1, \ell_2, \ell_3, L_2, n_2, n_3}^{KLM}(\Omega_p) &= [(Y_{\ell_1}(\widehat{\xi}_{1p})Y_{\ell_2}(\widehat{\xi}_{2p}))_{L_2} Y_{\ell_3}(\widehat{\xi}_{3p})]_{LM} \\ &\times \mathcal{P}_{n_2, n_3}^{\ell_1, \ell_2, \ell_3}(\varphi_{2p}, \varphi_{3p}),\end{aligned}\quad (5)$$

where

$$\begin{aligned}\mathcal{P}_{n_2, n_3}^{\ell_1, \ell_2, \ell_3}(\varphi_{2p}, \varphi_{3p}) &= \mathcal{N}_{n_2, n_3}^{\ell_1, \ell_2, \ell_3} (\sin \varphi_{2p})^{\ell_1} (\cos \varphi_{2p})^{\ell_2} \\ &\times (\sin \varphi_{3p})^{\ell_1 + \ell_2 + 2n_2} (\cos \varphi_{3p})^{\ell_3} \\ &\times P_{n_2}^{\ell_1 + \frac{1}{2}, \ell_2 + \frac{1}{2}}(\cos 2\varphi_{2p}) \\ &\times P_{n_3}^{\ell_1 + \ell_2 + 2n_2 + \ell_3 + \frac{1}{2}}(\cos 2\varphi_{3p})\end{aligned}\quad (6)$$

and $P_n^{a,b}$ are Jacobi polynomials. The coefficients $\mathcal{N}_{n_2, n_3}^{\ell_1, \ell_2, \ell_3}$ are normalization factors, given explicitly by the following:

$$\mathcal{N}_{n_2, n_3}^{\ell_1, \ell_2, \ell_3} = \prod_{j=2}^3 \left[\frac{2v_j \Gamma(v_j - n_j) n_j!}{\Gamma(v_j - n_j - \ell_j - 1/2) \Gamma(n_j + \ell_j + 3/2)} \right]^{\frac{1}{2}}, \quad (7)$$

where $v_j = K_j + (3j - 5)/2$ with K_j defined to be the following:

$$K_2 = \ell_1 + \ell_2 + 2n_2, \quad K_3 = K_2 + \ell_3 + 2n_3 \equiv K, \quad (8)$$

and K is the grand angular quantum number.

The HH functions are eigenfunctions of the hyperangular part of the kinetic energy operator Λ^2 . In fact, for $A = 4$ the latter operator can be written using the variables $\{\rho, \Omega_p\}$ as follows:

$$\sum_{j=1,3} \nabla_j^2 = \left[\frac{\partial^2}{\partial \rho^2} + \frac{8}{\rho} \frac{\partial}{\partial \rho} + \frac{\Lambda^2(\Omega_p)}{\rho^2} \right], \quad (9)$$

and

$$(\Lambda^2(\Omega_p) + K(K + 7))\mathcal{Y}_{\ell_1, \ell_2, \ell_3, L_2, n_2, n_3}^{KLM}(\Omega_p) = 0. \quad (10)$$

Another important property of the HH functions is that $\rho^K \mathcal{Y}_{\ell_1, \ell_2, \ell_3, L_2, n_2, n_3}^{KLM}(\Omega_p)$ are homogeneous polynomials of the particle coordinates of degree K .

The WF of a state with total angular momentum J , parity π and total isospin T can be expanded over the following complete basis of antisymmetrical hyperangular-spin-isospin states, defined as follows:

$$\Psi_{\mu}^{KLS TJ\pi} = \sum_{p=1}^{12} \Phi_{\mu}^{KLS TJ\pi}(i, j; k; m), \quad (11)$$

where the sum is over the 12 even permutations p and

$$\Phi_{\mu}^{KLS TJ\pi}(i, j; k; m) = \{ \mathcal{Y}_{\ell_1, \ell_2, \ell_3, L_2, n_2, n_3}^{KLM}(\Omega_p) [[[[s_i s_j]_{S_a} s_k]_{S_b} \times s_m]_S]_{J, J_z} [[[[t_i t_j]_{T_a} t_k]_{T_b} t_m]_{T, T_z} \}. \quad (12)$$

Here, $\mathcal{Y}_{\ell_1, \ell_2, \ell_3, L_2, n_2, n_3}^{KLM}(\Omega_p)$ is the HH state defined in Eq. (5) and s_i (t_i) denotes the spin (isospin) function of particle i . The total orbital angular momentum L of the HH function is coupled to the total spin S to give a total angular momentum J , J_z . The quantum number T specifies the total isospin, whereas $\pi = (-1)^{\ell_1 + \ell_2 + \ell_3}$ is the parity of the state. The integer index μ labels the possible choices of hyperangular, spin, and isospin quantum numbers, namely

$$\mu \equiv \{ \ell_1, \ell_2, \ell_3, L_2, n_2, n_3, S_a, S_b, T_a, T_b \}, \quad (13)$$

compatible with the given values of K, L, S, T, J , and π . Another important classification of the states is to group them into ‘‘channels’’: states belonging to the same channel have the same values of angular $\ell_1, \ell_2, \ell_3, L_2, L$, spin S_a, S_b, S and isospin T_a, T_b, T quantum numbers but different values of n_2, n_3 .

Each state $\Psi_{\mu}^{KLS TJ\pi}$ entering the expansion of the four-nucleon WF must be antisymmetric under the exchange of any pair of particles. Consequently, it is necessary to consider states such that

$$\Phi_{\mu}^{KLS TJ\pi}(i, j; k; m) = -\Phi_{\mu}^{KLS TJ\pi}(j, i; k; m). \quad (14)$$

Under the exchange $i \leftrightarrow j$, the Jacobi vector ξ_{3p} changes its sign, whereas ξ_{1p} and ξ_{2p} remain unchanged, and, therefore, the HH function $\mathcal{Y}_{\ell_1, \ell_2, \ell_3, L_2, n_2, n_3}^{KLM}(\Omega_p)$ transforms into itself times a factor $(-1)^{\ell_3}$ [see Eqs. (2) and (5)]. Conversely, the spin-isospin part transforms into itself times a factor $(-1)^{S_a + T_a}$ for the $i \leftrightarrow j$ exchange. Thus, the condition described by Eq. (14) is fulfilled when

$$\ell_3 + S_a + T_a = \text{odd}. \quad (15)$$

The number $M_{KLS TJ\pi}$ of the antisymmetrical functions $\Psi_{\mu}^{KLS TJ\pi}$ having given K, L, S, T, J , and π values but different combination of the quantum numbers indicated by μ is in general very large. In addition to the degeneracy of the HH basis, the four spins (isospins) can be coupled in different ways to S (T). However, many of the states $\Psi_{\mu}^{KLS TJ\pi}$ are linearly dependent among themselves. In the expansion of a four-nucleon WF it is necessary to include the linearly independent states only. To search for the independent states,

the essential ingredient is the knowledge of the matrix elements of the norm

$$N_{\mu\mu'}^{KLS TJ\pi} = \langle \Psi_{\mu}^{KLS TJ\pi} | \Psi_{\mu'}^{KLS TJ\pi} \rangle_{\Omega}, \quad (16)$$

where $\langle \rangle_{\Omega}$ denotes the evaluation of the spin-isospin traces and the integration over the hyperspherical variables.

The calculation of the above matrix elements, and also those of the Hamiltonian, is considerably simplified by using the following transformation:

$$\Phi_{\mu}^{KLS TJ\pi}(i, j; k; m) = \sum_{\mu'} a_{\mu, \mu'}^{KLS TJ\pi}(p) \Phi_{\mu'}^{KLS TJ\pi}(1, 2; 3; 4). \quad (17)$$

The coefficients $a_{\mu, \mu'}^{KLS TJ\pi}(p)$ have been obtained using the techniques described in Ref. [55]. The states $\Psi_{\mu}^{KLS TJ\pi}$ can be written as follows:

$$\Psi_{\mu}^{KLS TJ\pi} = \sum_{\mu'} A_{\mu, \mu'}^{KLS TJ\pi} \Phi_{\mu'}^{KLS TJ\pi}(1, 2; 3; 4), \quad (18)$$

where

$$A_{\mu, \mu'}^{KLS TJ\pi} = \sum_{p=1}^{12} a_{\mu, \mu'}^{KLS TJ\pi}(p). \quad (19)$$

The matrix elements of the norm can be easily obtained using the orthonormalization of the HH basis with the result that:

$$N_{\mu\mu'}^{KLS TJ\pi} = \sum_{\mu''} (A_{\mu, \mu''}^{KLS TJ\pi})^* A_{\mu', \mu''}^{KLS TJ\pi}. \quad (20)$$

Clearly,

$$\langle \Psi_{\mu}^{KLS TJ\pi} | \Psi_{\mu'}^{K'L'S'T'J'\pi'} \rangle_{\Omega} = 0, \quad (21)$$

if $\{KLS TJ\pi\} \neq \{K'L'S'T'J'\pi'\}$.

Once the quantities $N_{\mu\mu'}^{KLS TJ\pi}$ are calculated, the Gram-Schmidt procedure can be used, for example, to eliminate the linear-dependent states between the various $\Psi_{\mu}^{KLS TJ\pi}$ functions.

We have found that the number of independent states $M'_{KLS TJ\pi}$ for given K, L, S, T, J , and π is noticeably smaller than the corresponding value of $M_{KLS TJ\pi}$. To give an example, we have reported in Table I a few values of $M_{KLS TJ\pi}$ and $M'_{KLS TJ\pi}$ for the case $J = 0, T = 0, \pi = +$ corresponding to the ground state of the α particle. As can be seen from the table, the values of M_{KLL00+} are very large also for moderate values of K , but those for M'_{KLL00+} are usually much smaller.

The total WF of the four-nucleon bound state can finally be written as follows:

$$\Psi_4^{J\pi} = \sum_{KLS T} \sum_{\mu} \frac{u_{KLS T, \mu}(\rho)}{\rho^4} \Psi_{\mu}^{KLS TJ\pi}, \quad (22)$$

where the sum is restricted only to the linearly independent states. The expansion coefficients, which depend on the hyperradius, are determined by the Rayleigh-Ritz variational principle. By applying this principle, a set of second-order differential equations for the functions $u(\rho)$ are obtained. These equations and the procedure adopted to solve them has been outlined in the appendix of Ref. [56]. In this way, a large number of equation can be solved.

TABLE I. Number of four-nucleon antisymmetrical hyperspherical-spin-isospin states for the case $J = 0, T = 0$, and $\pi = +$ and the selected values of the grandangular quantum number K and total angular momentum L . $M_{KLSJT\pi}$ is the total number of the states defined in Eq. (11). $M'_{KLSJT\pi}$ gives the number of the linearly independent states with $\ell_1 + \ell_2 + \ell_3 \leq 6$. See the text for details.

K	$L = S = 0$		$L = S = 1$		$L = S = 2$	
	M_{K0000+}	M'_{K0000+}	M_{K1100+}	M'_{K1100+}	M_{K2200+}	M'_{K2200+}
0	2	1				
2	10	1	9	1	6	1
4	30	4	45	4	30	3
6	70	8	135	12	89	9
8	140	14	315	27	205	18
10	252	24	630	54	405	36
12	420	41	1,134	96	721	63
14	660	59	1,890	160	1,190	102
16	990	90	2,970	250	1,854	158
18	1,430	128	4,455	375	2,760	236
20	2,002	176	6,435	488	3,960	321
22	2,730	235	9,009	585	5,511	385
24	3,640	282	12,285	675	7,475	445
30	3,876		9,180		16,540	
40	10,626		26,565		47,145	
50	23,751		61,425		107,900	

The main problem is the computation of the matrix elements of the Hamiltonian. The kinetic energy operator matrix elements are readily calculated analytically, whereas the matrix elements of a local NN potential can be obtained by one-dimensional integrations. To this aim, it is convenient to write the basis in the jj coupling scheme as follows:

$$\Psi_{\mu}^{KLSJT\pi} = \sum_{\nu} B_{\mu,\nu}^{KLSJT\pi} \Xi_{\nu}^{KTJ\pi}(1, 2; 3; 4), \quad (23)$$

where

$$\begin{aligned} \Xi_{\nu}^{KTJ\pi}(1, 2; 3; 4) = & \{[(Y_{\ell_3}(\widehat{\xi}_3)(s_1 s_2)_{s_a})_{j_3} (Y_{\ell_2}(\widehat{\xi}_2)_{s_b})_{j_2}]_{J_2} \\ & \times (Y_{\ell_1}(\widehat{\xi}_1)_{s_4})_{j_1}\}_{JJ_z} [[t_i t_j]_{T_a} \\ & \times t_k]_{T_b} t_m]_{TT_z} \mathcal{P}_{n_2, n_3}^{\ell_1, \ell_2, \ell_3}(\varphi_{2p}, \varphi_{3p}), \quad (24) \end{aligned}$$

and $B_{\mu,\nu}^{KLSJT\pi}$ are related to the coefficients $A_{\mu,\mu'}^{KLSJT\pi}$ via Wigner $3j$ and $6j$ coefficients. Now, the integer index ν labels all possible choices of the

$$\nu \equiv \{n_3, \ell_3, S_a, j_3, n_2, \ell_2, j_2, J_2, \ell_1, j_1, T_a, T_b\}, \quad (25)$$

compatible with the given values of K, T, J , and π .

In terms of the states $\Xi_{\nu}^{KTJ\pi}(1, 2; 3; 4)$, it is easy to compute the matrix elements of an NN potential. For example, the matrix element of the isospin-conserving part $V_{IC}(1, 2)$ of the NN potential

$$\langle \Xi_{\nu}^{KTJ\pi}(1, 2; 3; 4) | V_{IC}(1, 2) | \Xi_{\nu'}^{K'T'J\pi}(1, 2; 3; 4) \rangle_{\Omega} = 0, \quad (26)$$

unless

$$\begin{aligned} & \{j_3, n_2, \ell_2, j_2, J_2, \ell_1, j_1, T_a, T_b, T\} \\ & = \{j'_3, n'_2, \ell'_2, j'_2, J'_2, \ell'_1, j'_1, T'_a, T'_b, T'\}. \quad (27) \end{aligned}$$

If Eq. (27) is verified, then

$$\begin{aligned} & \langle \Xi_{\nu}^{KTJ\pi}(1, 2; 3; 4) | V_{IC}(1, 2) | \Xi_{\nu'}^{K'T'J\pi}(1, 2; 3; 4) \rangle_{\Omega} \\ & = \mathcal{N}_{n_2, n_3}^{\ell_1, \ell_2, \ell_3} \mathcal{N}_{n_2, n_3}^{\ell'_1, \ell'_2, \ell'_3} \int_0^{\pi} d\varphi_3 (\cos \varphi_3)^{2+\ell_3+\ell'_3} \\ & \quad \times (\sin \varphi_3)^{5+2\ell_1+2\ell_2+4n_2} v_{\ell_3, S_a, \ell'_3, S'_a}^{j_3}(\rho \cos \varphi_3) \\ & \quad \times P_{n_3}^{\ell_1+\ell_2+2n_2+2, \ell_3+\frac{1}{2}}(\cos 2\varphi_3) \\ & \quad \times P_{n'_3}^{\ell'_1+\ell'_2+2n_2+2, \ell'_3+\frac{1}{2}}(\cos 2\varphi_3), \quad (28) \end{aligned}$$

where $v_{\ell, S, \ell', S'}^j(r)$ is the isospin-conserving part of the NN potential acting between two-body states $^{2S+1}(\ell)_j$ and $^{2S'+1}(\ell')_j$. The one-dimensional integral given in Eq. (28) can be computed numerically with high accuracy. The case of the isospin-breaking part of the NN interaction is a generalization of the previous case: now we can have $\{T_a, T_b, T\} \neq \{T'_a, T'_b, T'\}$ as well.

The $3N$ interaction matrix elements are more difficult to compute and the adopted procedure is detailed in Appendix A.

III. CHOICE OF THE BASIS

The main difficulty of applying the HH technique is the selection of a restricted and effective subset of basis states. In fact, although the number of independent states proves to be much smaller than the degeneracy $M_{KLSJT\pi}$ of the basis, the brute force application of the method, that is, the inclusion of all HH states having $K \leq K_M$ in the expansion and then increasing K_M until convergence, would be destined to fail. In fact, because of the strong correlations induced by the NN potential, $K_M \approx 60$ are necessary to obtain a good convergence. However, even for values of $K > 20$ it is very difficult to find the linearly independent states via the Gram-Schmidt procedure because the loss of precision in the orthogonalization procedure.

It is convenient to separate the HH functions into classes having particular properties and advantageously take into account the fact that the convergence rates of the various classes are rather different. As discussed in the Introduction, we expect that the contribution of the HH functions describing the two-body correlations to be very important [48]. Another criterion adopted is first to consider the HH functions with low values of ℓ_i .

An important quantity in the choice of the classes is $\mathcal{M}_i(K_i)$, namely the number of linearly independent antisymmetrical spin-isospin-HH states $\Psi_{\mu}^{KLSJT\pi}$ belonging to a class i and having $K \leq K_i$. Only even parity states have been included in the construction of the α -particle WF, and thus the discussion hereafter will be limited to consider only even values for K_i . In general, for a class i , the value $\mathcal{M}_i(K_i)$ is zero for $K_i < K_i^a$, because of the fact that the linearly dependent states have been removed from the expansion. For example,

TABLE II. Quantum numbers of the first channels considered in the expansion of the α -particle WF. See the text for details.

α	ℓ_1	ℓ_2	ℓ_3	L_2	L	S_a	S_b	S	T_a	T_b	T
1	0	0	0	0	0	1	1/2	0	0	1/2	0
2	0	0	0	0	0	0	1/2	0	1	1/2	0
3	0	0	2	0	2	1	3/2	2	0	1/2	0
4	1	1	0	0	0	1	1/2	0	0	1/2	0
5	1	1	0	0	0	0	1/2	0	1	1/2	0
6	1	1	0	1	1	1	1/2	1	0	1/2	0
7	1	1	0	1	1	1	3/2	1	0	1/2	0
8	1	1	0	1	1	0	1/2	1	1	1/2	0
9	0	2	0	2	2	1	3/2	2	0	1/2	0
10	2	0	0	2	2	1	3/2	2	0	1/2	0
11	1	1	0	2	2	1	3/2	2	0	1/2	0
12	1	0	1	1	0	1	1/2	0	1	1/2	0
13	1	0	1	1	0	0	1/2	0	0	1/2	0
14	0	1	1	1	0	1	1/2	0	1	1/2	0
15	0	1	1	1	0	0	1/2	0	0	1/2	0
16	1	0	1	1	1	1	1/2	1	1	1/2	0
17	1	0	1	1	1	1	3/2	1	1	1/2	0
18	1	0	1	1	1	0	1/2	1	0	1/2	0
19	0	1	1	1	1	1	1/2	1	1	1/2	0
20	0	1	1	1	1	1	3/2	1	1	1/2	0
21	0	1	1	1	1	0	1/2	1	0	1/2	0
22	1	0	1	1	2	1	3/2	2	1	1/2	0
23	0	1	1	1	2	1	3/2	2	1	1/2	0

as should be clear by inspection of Table I, there is only one linearly independent state Ψ_{μ}^{KLS00+} with $K = 0$. If this state is included in the first class, the other classes must have at least $K_i^a = 2$, etc. For $K_i \gg K_i^a$, $\mathcal{M}_i(K_i)$ reaches a sort of “asymptotic” value, given by $\mathcal{M}_i(K_i) \approx M_i \times (K_i)^{r_i}$. The choice of the classes has clearly to be optimized so that the convergence for the classes with large values of M_i and r_i could be reached for relatively low values of K . The specific values of M_i and r_i are discussed below.

To study the α -particle ground state we have found very convenient to choose the classes as follows:

- Class C1. In this class the $T = 0$ HH states belonging to the PB are included. For $A = 4$, the PB includes states of the first three channels reported in Table II (the only channels with $\ell_1 = \ell_2 = 0$) having $n_2 = 0$. As can be seen from Eq. (5), the corresponding states depend only on $\widehat{\xi}_{3p}$ and $\cos \varphi_{3p} = \xi_{3p}/\rho \equiv r_{ij}/\rho$ and therefore contain only two-body correlations. For this class, $K_1^a = 0$. For $K_1 \geq 4$, $\mathcal{M}_1(K_1) = (3/2)K_1$. Then, this is a “small” class. As shown in the next section, this is also the most slowly convergent class, but because $M_1 = (3/2)$ and $r_1 = 1$, it is not difficult to reach the desired degree of accuracy. In the present calculation, states up to $K_1 = 72$ have been included.
- Class C2. This class includes the $T = 0$ states belonging to the same three channels as those of class C1, but with $n_2 > 0$. These states therefore include also part of the three-body correlations. The first linearly independent states of this class appear for $K = 4$, therefore $K_2^a = 4$. Moreover, $\mathcal{M}_2(K_2) = (3/4)(K_2)^2 + \mathcal{O}(K_2)$ for $K_2 \gg 1$. This can be

considered a “small” class, too, and states up to $K_2 = 40$ have been included in the present calculation without difficulty.

- Class C3. This class includes the remaining $T = 0$ states of the channels having $\ell_1 + \ell_2 + \ell_3 = 2$. The corresponding 20 possible channels are reported in Table II in rows 4–23. In this case $K_3^a = 2$ and $\mathcal{M}_3(K_3) = 5(K_3)^2 + \mathcal{O}(K_3)$ for $K_3 \gg 1$. This is a fairly “large” class, but with the necessary care states with $K_3 \approx 34$ can be still included in the expansion.
- Class C4. This class includes $T = 0$ states belonging to the channels with $\ell_1 + \ell_2 + \ell_3 = 4$. There are 57 channels of this kind. In this case $K_4^a = 8$ and it follows that $\mathcal{M}_4(K_4) = (57/4)(K_4)^2 + \mathcal{O}(K_4)$ for $K_4 \gg 1$. This is a “large” class, but its contribution to the α -particle BE, though still sizable, is by far less important than the first three classes. States of up to $K_4 \approx 28$ have been considered.
- Class C5. This class includes $T = 0$ states belonging to the channels with $\ell_1 + \ell_2 + \ell_3 = 6$. There are 109 channels of this kind. In this case $K_5^a = 12$ and for $K_5 \gg 1$ we have $\mathcal{M}_5(K_5) = (109/4)(K_5)^2 + \mathcal{O}(K_5)$. This is a very “large” class, but it contributes very little to the α -particle BE, as we shall see. Therefore, we can truncate the expansion already at $K_5 \approx 20$.
- Class C6. This class includes the states having $T > 0$. We have included in the expansion all the channels of this kind with $\ell_1 + \ell_2 + \ell_3 \leq 2$ (45 channels). In this case $K_6^a = 0$ and for $K_6 \gg 1$ we have $\mathcal{M}_6(K_6) = (45/4)(K_6)^2 + \mathcal{O}(K_6)$. Also the contribution of this class to the BE is very tiny, and states up to $K_6 = 16$ have been included in the expansion.

The states belonging to the classes C2 and C3 describe the most important three-body contributions to the WF. The classes C4 and C5 take into account the remaining three- and four-body correlations ordered with increasing values of $\ell_1 + \ell_2 + \ell_3$.

The convergence is studied as follows. First, only the states of class C1 with $K \leq K_1$ are included in the expansion and the convergence of the BE is studied as the value of K_1 is increased. Once a satisfactory value of $K_1 = K_{1M}$ is reached, the states of the second class with $K \leq K_2$ are added to the expansion, keeping all the states of the class C1 with $K \leq K_{1M}$. Then K_2 is increased up to K_{2M} to reach the desired convergence for the BE. With some extra work, it is possible at this point to optimize the basis by removing some of the $K \leq K_{2M}$ states of class C2 that give very tiny contributions to the BE. The procedure outlined is then repeated for each new class. Our complete calculation includes about 8000 HH states.

It should be noticed that in the present calculation only HH functions constructed in terms of the Jacobi vectors given in Eq. (3), referred to as the set A, have been considered. As is well known, there is another possible choice, namely

$$\begin{aligned}
 \xi'_{1p} &= \mathbf{r}_m - \mathbf{r}_k, \\
 \xi'_{2p} &= \sqrt{\frac{1}{2}}(\mathbf{r}_k + \mathbf{r}_m - \mathbf{r}_i - \mathbf{r}_j), \\
 \xi'_{3p} &= \mathbf{r}_j - \mathbf{r}_i,
 \end{aligned} \tag{29}$$

TABLE III. List of the parameters of the central NN potentials used in this article. Each potential $V(r)$ is given by $V(r) = \sum_i V_i f(\mu_i, r)$, where the function $f(\mu_i, r)$ is either $\exp(-\mu_i r^2)$ for the Gaussian potentials or $\exp(-\mu_i r)/r$ for the Yukawa potentials. The operators V_i act on the spin-isospin degrees of freedom and are written as $V_i = \bar{V}_i \times (W_i + B_i P_\sigma - H_i P_\tau + M_i P_r)$, where P_σ , P_τ , and P_r are the spin-, isospin-, and space-exchange operators. The potential strengths \bar{V}_i are in units of MeV for Gaussian-type and MeV fm for Yukawa-type potentials, respectively. The parameters W_i , M_i , B_i , and H_i are dimensionless and the ranges μ are in units of fm^{-2} for Gaussian-type or fm^{-1} for Yukawa-type potentials, respectively. The Majorana mixture parameter M of the Volkov potential is set to 0.6 in the calculation. The parameter u in the Minnesota parameter is set to unity in the calculation.

Potential	Type	i	\bar{V}_i	μ_i	W_i	M_i	B_i	H_i
MT-V [49]	Yukawa	1	1458.047	3.11	1.0	0.0	0.0	0.0
		2	-578.089	1.55	1.0	0.0	0.0	0.0
MT I/III [49]	Yukawa	1	1438.72	3.11	1.0	0.0	0.0	0.0
		2	-570.4255	1.55	1.0	0.0	0.0	0.0
		3	-56.4585	1.55	0.0	0.0	1.0	0.0
Volkov [64]	Gauss	1	144.86	0.82^{-2}	$1.0 - M$	M	0.0	0.0
		2	-83.34	1.60^{-2}	$1.0 - M$	M	0.0	0.0
ATS3 [65]	Gauss	1	1000.0	3.0	1.0	0.0	0.0	0.0
		2	-326.7	1.05	0.5	0.0	0.5	0.0
		3	-166.0	0.80	0.5	0.0	-0.5	0.0
		4	-43.0	0.60	0.5	0.0	0.5	0.0
		5	-23.0	0.40	0.5	0.0	-0.5	0.0
Minnesota [66]	Gauss	1	200.0	1.487	$0.5u$	$1.0 - 0.5u$	0.0	0.0
		2	-178.0	0.639	$0.25u$	$0.5 - 0.25u$	$0.25u$	$0.5 - 0.25u$
		3	-91.85	0.465	$0.25u$	$0.5 - 0.25u$	$-0.25u$	$-0.5 + 0.25u$

hereafter referred as the set B of Jacobi vectors. Considering, for example, the α -particle ground state, the HH functions $\mathcal{Y}_{\text{set A}}$ of the set A are more appropriate for describing those contributions to the WF corresponding to $\{3 + 1\}$ clustering structures, namely ${}^3\text{He} + n$ or ${}^3\text{H} + p$. The HH functions $\mathcal{Y}_{\text{set B}}$ constructed with the set B, should be more suitable for describing the $\{2 + 2\}$ clustering structures, such as the $d + d$ configurations. It is rather obvious that the inclusion of HH functions of both sets should speed up the convergence in constructing the full state of the system [29,40]. If the expansion of the WF is done over only a particular set, those configurations in which other clustering structures are important would be generally described with difficulty and a slow convergence would result.

In the present calculation we have included HH states $\mathcal{Y}_{\text{set A}}$ only, that is, constructed with the Jacobi vectors of the set A, because this has been found to be sufficient to reach the desired degree of convergence. In fact, the full basis considered (classes C1–C6) is large enough to include all the possible independent states for $K \leq 20$. Additional linearly independent states constructed with the set B would appear only for $K \geq 22$. As clarified below, the contribution of states with $K \geq 22$ not belonging to classes C1–C3 is rather small. Therefore, in the present calculation it is not necessary to introduce states of the set B. However, in the present formalism there would be no particular difficulty in also including states constructed with the set B.

IV. RESULTS FOR THE α -PARTICLE GROUND STATE

In this section, the results obtained for the ground state of the α particle are presented. The convergence of the HH

expansion in terms of the various classes is examined in Sec. IV A. The results obtained for the BE and other ground-state properties for a number of different interaction models are reported in Sec. IV B. The origin of the $T > 0$ components in the α -particle ground state is discussed in Sec. IV C. The effect of the truncation of the NN and $3N$ interactions is studied in Sec. IV D. The calculation of the various ${}^4\text{He}$ asymptotic normalization constants is considered in Sec. IV E. Finally, some details of the practical implementation of the method are discussed in Sec. IV F.

A. Convergence of the HH expansion

To study the convergence of the HH expansion, we have considered three different interaction models frequently used in literature. The first calculation has been performed using the MT-V potential [49], a central spin-independent interaction. The parameters defining this potential has been reported in Table III for completeness. We have used in this work $\hbar^2/m = 41.47 \text{ MeV fm}^2$. This potential has been used for a number of benchmarks. It does not contain noncentral components, but it retains a rather strong repulsion at short interparticle distance going like $1/r$. It is therefore rather challenging for a technique where the correlations are not built in. In the second example, we have considered the AV18 potential model [5], which represents a NN interaction in its full richness, with short-range repulsion, tensor and other noncentral components, charge symmetry breaking terms, and Coulomb and other electromagnetic interactions. In the third case, we have added to the AV18 potential the Urbana IX model [2] of $3N$ interaction (AV18+UIX model). For the latter two models we have used $\hbar^2/m = 41.47108 \text{ MeV fm}^2$.

TABLE IV. Convergence of α -particle binding energies (MeV) corresponding to the inclusion in the WF of the different classes C1–C6 in which the HH basis has been subdivided.

K_1	K_2	K_3	K_4	K_5	K_6	MT-V	AV18	AV18 + UIX
20						28.928	14.701	14.902
30						29.794	15.992	16.162
40						29.962	16.172	16.337
50						30.008	16.205	16.369
60						30.024	16.213	16.377
70						30.032	16.214	16.379
72						30.033	16.214	16.379
72	8					30.714	18.286	18.985
72	16					31.170	19.755	20.645
72	24					31.240	19.967	20.865
72	32					31.256	20.014	20.909
72	36					31.259	20.022	20.916
72	40					31.261	20.026	20.919
72	40	8				31.300	21.940	24.682
72	40	16				31.336	23.237	27.142
72	40	24				31.340	23.371	27.350
72	40	30				31.341	23.385	27.370
72	40	34				31.341	23.388	27.373
72	40	34	8			31.341	23.525	27.553
72	40	34	16			31.344	24.086	28.312
72	40	34	20			31.346	24.145	28.382
72	40	34	24			31.347	24.163	28.404
72	40	34	28			31.347	24.170	28.414
72	40	34	28	16			24.181	28.427
72	40	34	28	20			24.191	28.439
72	40	34	28	24			24.195	28.444
72	40	34	28	24	4		24.205	28.456
72	40	34	28	24	8		24.209	28.461
72	40	34	28	24	12		24.210	28.462
72	40	34	28	24	16		24.210	28.462
"exact"						31.359	24.25	28.50

We study the convergence as explained in the previous section, and the results presented in Table IV are arranged accordingly. For example, the BE B reported in a row with a given set of values of K_1, \dots, K_6 has been obtained by including in the expansion all the HH functions of class C_i with $K \leq K_i, i = 1, \dots, 6$.

For the MT-V potential, we observe a slow convergence of the classes C1 and C2 and fairly large values of K have to be used. Conversely, they give 96% of the total BE. The contributions of the other classes are extremely small. The class C3 increases the BE by an additional 0.08 MeV and the class C4 by less than 0.01 MeV. Class C5 gives a negligible contribution, and class C6 has not been included in the expansion because for this potential isospin is a good quantum number and there is no mixing with $T > 0$ components. The final value $B = 31.347$ MeV is in good agreement with the results found in the literature, whose "average" (based on the results reported in Refs. [26,29,33,58] is reported in the last row of Table IV. There is approximately 10 keV of missing energy because of the truncation of our expansion as discussed at the end of this subsection.

For the AV18 potential, the first two classes give important contributions but a large amount of BE is still missing. The inclusion of the third class increases the BE by more than 3 MeV but 0.8 MeV are still missing. Because the second and third classes take into account a large part of the contributions of the three-body correlations, this means that also the four body correlation is important. These are related to the configurations where the clusterization $2 + 2$ is important. In our calculation, such configurations are included when the classes C4 and C5 are taken into account. The number of the states of class C4 increases very rapidly with K_4 but fortunately the convergence is reached around $K = 24$. The gained BE is almost 0.8 MeV. There are no linearly independent states of class C5 with $K < 14$ and its contribution is rather small. The convergence is again obtained around $K = 24$, but the gain in energy is only about 0.02 MeV. Because the number of states of this class is very large, for example, $\mathcal{M}_6(20) \approx 800$ when confronted with a very tiny gain in BE, a selection of the states has to be performed to save computing time and to avoid loss of numerical precision. For example, all the channels of class C5 with a total orbital angular momentum $L = 0$ have

not been included in the expansion because their contribution is absolutely negligible. With their inclusion the procedure of Ref. [56] for finding the eigenvalue would become numerically instable.

From Table IV, one can try to estimate the contribution of the states with $\mathcal{L} = \ell_1 + \ell_2 + \ell_3 = 8$. From the previous discussion we have already seen that the states having $\mathcal{L} = 4$ (class C4) contribute by about 0.8 MeV, whereas the states with $\mathcal{L} = 6$ (class C5) contribute by less than 0.03 MeV. Therefore, the states with $\mathcal{L} = 8$ are expected to give a negligible contribution to the α -particle BE. Finally, the inclusion of states with $T > 0$ (class C6) increases the BE by another 20 keV, approximately.

The convergence rate when considering the UIX $3N$ interaction is similar to the AV18 case. The corresponding results are reported in the last column of Table IV (they have been obtained in the approximation described in Sec. IV D). Because the models most frequently used for the $3N$ interactions are rather soft at short interparticle distances, the convergence rate of the C1 and C2 classes does not change appreciably. However, the $3N$ potential has a very strong state dependence and the convergence of the C3–C5 classes are now slightly slower. For example, the gain in BE of the C4 class is about 0.8 MeV without any $3N$ interactions, and it becomes about 1 MeV when including the $3N$ interaction. Our final results for the AV18 and AV18+UIX models agree well with the FY results of Ref. [24] reported in the last row of Table IV. The convergence properties for other NN and $NN+3N$ potential models has been found rather similar to those showed in Table IV.

Finally, let us comment about the convergence rate of the expansion as a function of the maximal grand angular quantum numbers K_i of the various classes of HH states included in our expansion. Previous studies [47,48,59,60] have shown that the trend of convergence toward the exact BE depends primarily on the form of the potential. In particular, for potentials that are given as functions of r_{ij}^2 (as, for example, those given as a sum of Gaussians) the increase of BE with K_i diminishes exponentially. Conversely, for potentials given as a function of r_{ij} (as a sum of exponentials or Yukawians), the increase of BE decreases as $(1/K_m)^p$, where p is a positive integer number. The value of p is smaller for potentials of Yukawa type because of the $1/r$ divergence at the origin but may depend also on the class of the HH functions whose convergence is studied. It is important to determine the value of K_m at which the convergence starts to behave as stated previously. The asymptotic behavior of the convergence should be reached for HH functions whose kinetic energy $\propto (\hbar^2/m)K(K+7)/\rho_0^2$ is much greater than the BE, where ρ_0 is a value of the hyperradius ρ for which $\Psi(\rho_0)$ can be regarded as small [47]. In our studies, we have found that the asymptotic falling starts at $K_m \approx 30 \div 40$.

To study the convergence behavior we have indicated with $B(K_1, K_2, K_3, K_4, K_5, K_6)$ the BE obtained by including in the expansion all the HH states of the class C1 with $K \leq K_1$, all the HH states of the class C2 having $K \leq K_2$, and so on. Let us compute

$$\Delta_1(K) = B(K, 0, 0, 0, 0, 0) - B(K-2, 0, 0, 0, 0, 0), \quad (30)$$

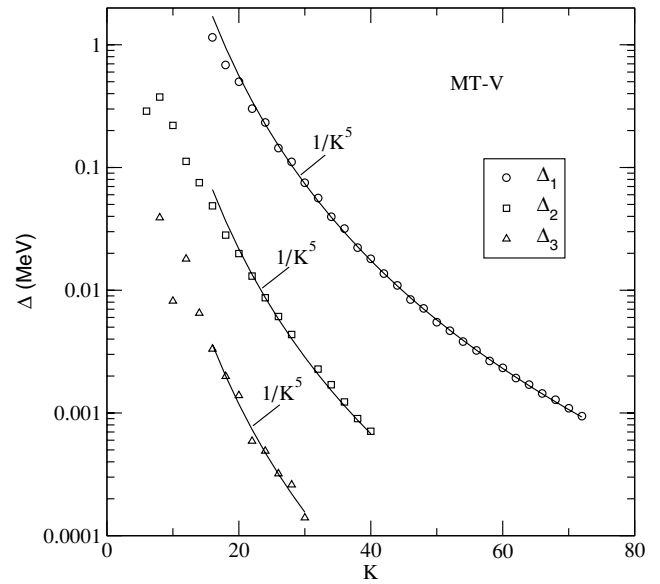


FIG. 1. Binding energy differences for the α particle for the classes C1 (circles), C2 (squares), and C3 (triangles) as function of the grand angular value K (see the text for more details). The potential used is the MT-V. The curves are fitted to the large K part of the energy differences.

$$\Delta_2(K) = B(K_{1M}, K, 0, 0, 0, 0) - B(K_{1M}, \times K - 2, 0, 0, 0, 0), \quad K_{1M} = 72, \quad (31)$$

$$\Delta_3(K) = B(K_{1M}, K_{2M}, K, 0, 0, 0) - B(K_{1M}, K_{2M}, \times K - 2, 0, 0, 0), \quad K_{2M} = 40, \quad (32)$$

and so on. The values obtained for Δ_i , $i = 1, 3$ are shown in Fig. 1 for the MT-V potential model, together with the curves $(1/K)^p$ for $p = 5$ [the curves have been normalized to fit the high K part of the $\Delta_{1,3}(K)$ values]. As can be seen in Fig. 1, all the energy differences Δ_1 , Δ_2 , and Δ_3 decrease as $1/K^5$ for $K \geq 20$, approximately. However, for a given K , there is a clear hierarchy $\Delta_1(K) \gg \Delta_2(K) \gg \Delta_3(K)$. Note that there are slight fluctuations in the $\Delta(K)$ as K is increased (this is evident in particular for Δ_3).

The values obtained for Δ_i , $i = 1, 4$ for the AV18 potential are reported in Fig. 2. The decrease of Δ_1 , Δ_3 , and Δ_4 clearly follows a law $(1/K)^p$ with $p = 7$. The behavior of the energy difference Δ_2 can be approximated either by a $1/K^6$ or a $1/K^7$ law. The faster decrease of these results compared to the previous case is because of the fact that the AV18 potential does not diverge at the origin, whereas the MT-V has a $1/r$ divergence. The study of Ref. [47], in fact, predicts a difference of two units in the exponential coefficient for the two cases (Yukawian potentials vs. regular potentials). For fixed K , also for the AV18 we note a systematic hierarchy $\Delta_1(K) \gg \Delta_2(K) \gg \Delta_3(K) \gg \Delta_4(K)$, although less pronounced than in the MT-V case. The same behavior is observed when the UIX $3N$ potential is included.

From the observed simple behavior, we can readily estimate the missing BE due to the truncation of the expansion to finite values of $K = \bar{K}$. Let us suppose that the states of class i up to $K = \bar{K}$ have been included and to have computed $\Delta_i(\bar{K})$.

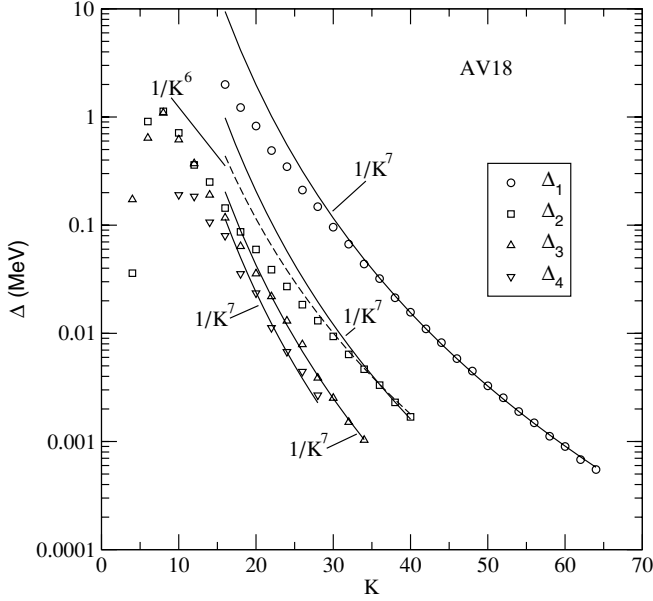


FIG. 2. Binding energy differences for the α particles for the classes C1 (circles), C2 (squares), C3 (up triangles), and C4 (down triangles) as function of the grand angular value K (see the text for more details). The potential used is the AV18. The curves are fitted to the large K part of the energy differences.

Then, the missing BE due to the states with $K = \bar{K} + 2, \bar{K} + 4, \dots$, is given by the following:

$$(\Delta B)_i = c(\bar{K}, p) \Delta_i(\bar{K}), \quad c(\bar{K}, p) = \sum_{K=\bar{K}+2, \bar{K}+4, \dots}^{\infty} \left(\frac{\bar{K}}{K} \right)^p, \quad (33)$$

where $c(\bar{K}, p)$ is a numerical coefficient. For example, let us consider the “missing” energy for the Class C1 in the MT-V case. In this case $\bar{K} = 72$ and $p = 5$ and $c(72, 5) = 8.51$. Because $\Delta_1(\bar{K} = 72) = 0.99$ keV, we find that $\Delta B_1 = 8.4$ keV. Adding this value to $B(72, 0, 0, 0, 0, 0)$ we can extrapolate the BE for the case of the inclusion of the *whole* class C1: $B(72, 0, 0, 0, 0, 0) + (\Delta B)_1 \approx 30.041$ MeV. The BE obtained corresponding to this case (converged PB expansion) has been computed very precisely in Ref. [61] using a “pair-correlated”

potential basis (PPB). In such an expansion, each PB function is multiplied by a pair correlation factor and this allows for a very rapid convergence of the expansion. In that article, we found $B(\text{PPB}) = 30.042$ MeV, which agrees very well with the above extrapolated value. To reach such a value, it would be necessary to use $\bar{K} \approx 150$ for the class C1.

For the AV18, we find $c(72, 7) = 5.52$, $\Delta_1(\bar{K} = 72) = 0.24$ keV and therefore $(\Delta B)_1 \approx 1.3$ keV, a rather tiny quantity. Because of the faster convergence for this potential like $1/K^7$, it does not seem necessary to increase K_1 any further in this case.

The “missing” energy of the other classes can be estimated in the same way. However, to estimate the “missing” energy for the whole calculation due to the truncation of the expansion of the first class up to $K \leq K_1$, of the second class up to $K \leq K_2$, and so on, we cannot simply add the $(\Delta B)_i$, $i = 1, \dots, 6$ so obtained. The reason is that, for example, the inclusion of the HH states of classes C2, C3, \dots , also alters the convergence of class C1, and so on by a small amount. To study the “full” rate of convergence, let us consider the following:

$$\begin{aligned} \bar{\Delta}_1(K) &= B(K, K_{2M}, K_{3M}, K_{4M}, K_{5M}, K_{6M}) \\ &\quad - B(K-2, K_{2M}, K_{3M}, K_{4M}, K_{5M}, K_{6M}), \\ \bar{\Delta}_2(K) &= B(K_{1M}, K, K_{3M}, K_{4M}, K_{5M}, K_{6M}) \\ &\quad - B(K_{1M}, K-2, K_{3M}, K_{4M}, K_{5M}, K_{6M}), \\ \bar{\Delta}_3(K) &= B(K_{1M}, K_{2M}, K, K_{4M}, K_{5M}, K_{6M}) \\ &\quad - B(K_{1M}, K_{2M}, K-2, K_{4M}, K_{5M}, K_{6M}), \end{aligned} \quad (34)$$

and so on. Clearly $\Delta_6(K) \equiv \bar{\Delta}_6(K)$. The differences between $\Delta_i(K)$ and $\bar{\Delta}_i(K)$ for $i = 2 \div 5$ have been found to be negligible. Only the differences between $\Delta_1(K)$ and $\bar{\Delta}_1(K)$ are sizable. In any case the behavior of $\bar{\Delta}_i(K)$ for large K is the same as that discussed for $\Delta(K)$. Therefore, we propose to estimate the “total missing” BE by using the formula

$$(\Delta B)_T = \sum_{i=1,6} c(K_{iM}, p) \bar{\Delta}_i(K_{iM}), \quad (35)$$

where $p = 5$ (7) for the MT-V potential (AV18 and AV18+UIX). To give an example, the values for $\Delta_i(K_{iM})$ and $c(K_{iM}, p)$ computed for the MT-V case are reported in Table V, from which it is possible to derive that $(\Delta B)_T \approx 11$ keV.

TABLE V. Increments of the α -particle BE $\bar{\Delta}(K)$, computed using Eq. (34) for the various classes $i = 1, \dots, 6$ and the MT-V and AV18 potential models. The quantities $c(K, p)$ are defined in Eq. (33) and $(\Delta B)_i$, given by $c(k, p) \bar{\Delta}_i(k)$, represents the “missing BE” for having truncated the expansion over the class i up to the given value of $K = K_M$. Finally, the “total missing BE” $(\Delta B)_T$ is computed from Eq. (35).

i	MT-V				AV18		
	K_M	$\bar{\Delta}_i(K)$ [keV]	$c(K, 5)$	$(\Delta B)_i$ [keV]	$\bar{\Delta}_i(K)$ [keV]	$c(K, 7)$	$(\Delta B)_i$ [keV]
1	72	0.89	8.51	7.57	0.10	5.52	0.55
2	40	0.71	4.52	3.21	0.91	2.86	2.60
3	34	0.07	3.77	0.26	1.16	2.37	2.75
4	28	0.13	3.03	0.39	2.30	1.87	4.30
5	24	—	—	—	1.47	1.54	2.26
$(\Delta B)_T$				11.43			12.46

TABLE VI. The α -particle binding energies B (MeV), rms radii (fm), and expectation value $\langle K \rangle$ of the kinetic energy operator (MeV) for various central interaction models as computed by means of the HH expansion are compared with the results obtained by other techniques. The binding energies obtained by using the extrapolation technique described in Sec. IV A are enclosed in parentheses.

Interaction	Method	B	$\langle r^2 \rangle^{1/2}$	$\langle K \rangle$
Volkov	HH (this work)	30.420	1.490	50.319
	SVM [26]	30.424	1.49	
	HH [45]	30.399		
ATS3	HH (this work)	31.618	1.412	74.366
	SVM [62]	31.616	1.42	
Minnesota	HH (this work)	29.947	1.4105	58.086
	SVM [26]	29.937	1.41	
	EIHH [33]	29.964	1.4106	
MT-V	HH (this work)	31.347(31.358)	1.4081	69.792
	SVM [26]	31.360	1.4087	
	EIHH [33]	31.358	1.40851	
	CRCG [29]	31.357		
	FY [58]	31.364		
	ATMS [63]	31.364	1.40	
MT-I/III	HH (this work)	30.310(30.331)	1.4380	66.180
	FY [22]	30.312		

If this value is added to $B(72, 40, 34, 28, 0, 0) = 31.347$ MeV, we obtain 31.358 MeV, which is in very good agreement with the results obtained by other groups. For the AV18 potential, Eq. (35) gives $(\Delta B)_T = 12$ keV, and if this value is added to $B(72, 40, 34, 28, 24, 16) = 24.210$ MeV, we obtain 24.222 in close agreement with the FY estimates of 24.25 MeV of Ref. [24] and 24.223 of Ref. [11]. Note that for the class C2 we have computed the coefficient $c(\bar{K}, p)$ with $p = 7$. Using $p = 6$, we have $c(40, 6) = 3.52$ and $(\Delta B)_2 = 3.20$ keV (instead of 2.60 keV), a very small change. For the AV18+UIX model, the same procedure allows for an extrapolated BE estimate of 28.474 MeV, again in agreement with the FY value 28.50 MeV. Note that the FY BE results are quoted with an

uncertainty of 50 keV due to the truncated model space in their calculations [24].

B. Results for different NN and $3N$ potentials

The BE values obtained for a number of different potential models after including the states of the 6 different classes up to the values $K_1 = 72, K_2 = 40, K_3 = 34, K_4 = 28, K_5 = 24$, and $K_6 = 16$ (the last two values only for the realistic cases, for central potential we have taken $K_5 = K_6 = 0$) are presented in Tables VI and VII. Table VI presents the results for some central potential models, whereas Table VII reports the results for various realistic potentials with and without

TABLE VII. The α -particle binding energies B (MeV), the rms radii (fm), the expectation values of the kinetic energy operator $\langle K \rangle$ (MeV), and the P and D probabilities (%) for various realistic interaction models as computed by means of the HH expansion are compared with the results obtained by other techniques. The binding energies obtained by using the extrapolation technique described in Sec. IV A are enclosed in parentheses.

Interaction	Method	B	$\langle K \rangle$	$\langle r^2 \rangle^{1/2}$	P_P	P_D
AV18	HH (this work)	24.210(24.222)	97.84	1.512	0.347	13.74
	FY [24]	24.25	97.80			
	FY [11]	24.223	97.77			
Nijm II	HH (this work)	24.419(24.432)	100.27	1.504	0.334	13.37
	FY [24]	24.56	100.31			
AV18+UIX	HH (this work)	28.462(28.474)	113.30	1.428	0.73	16.03
	FY [24]	28.50	113.21			
	GFMC [4]	28.34(4)	110.7(7)			
AV18+TM'	HH (this work)	28.301(28.313)	110.27	1.435	0.73	15.63
	FY [24]	28.36	110.14			

including different models for the $3N$ forces, too. The BE's obtained by using the extrapolation technique described in the previous section are enclosed in parentheses. Results obtained by other techniques are also reported.

Let us consider first the central potentials (for all of them we have taken $\hbar^2/m = 41.47 \text{ MeV fm}^2$). We have selected five different potential models, that is, the Volkov [64], the Afnan-Tang S3 (ATS3) [65], the Minnesota [66], the MT-V, and the Malfliet-Tjon version I/III (MT-I/III) [49]. These potentials have been used by several groups to produce benchmark calculations, but unfortunately for each of them different versions exist. For that reason, we have reported the parameters of the potentials used in the present work in Table III. Note that the first four potentials mentioned above are equal to those used in Ref. [26], whereas the version of the MT-I/III used is the same as reported in Table I of Ref. [22]. The Volkov and MT-V are spin independent, whereas the other three potentials are spin dependent. It is customary to include the point-Coulomb interaction ($e^2 = 1.44 \text{ MeV fm}$) with the Minnesota potential, whereas the MT-I/III version acts only on S waves. Clearly for this group of potentials, the total orbital angular momentum is a good quantum number and therefore we have included in the WF's only the channels with $L = 0$.

The first example is the Volkov potential with Majorana parameter $M = 0.6$. As can be seen in Table VI, our result agrees very well with the estimates by other techniques, especially with the one using the SVM [26]. The Volkov potential, given as a sum of Gaussians, has a very soft core and therefore the induced two-body correlations in the ground state WF are weaker than in the other cases. In fact, we have found that the convergence of the HH expansion is in this case much faster (it is reached for $K_1 \approx 30$). Because inclusion of HH states with fairly low values of the grand angular quantum number are sufficient to obtain convergence, a successful HH calculation for this potential was already possible 20 years ago [45].

Others central potentials often used in the literature are the ATS3 and Minnesota potentials. Both are given as a sum of Gaussians but have a rather strong repulsion at short interparticle distances. This induces important two-body correlations in the WFs and consequently an acceptable convergence for the first class is reached only for $K_1 > 40$. The chosen version of the Minnesota potential has the exchange parameter $u = 1$. As mentioned before, the point-Coulomb potential is included in the calculation; however, in the WF we have included only states with $T = 0$. In both cases, we observe a good agreement between the different theoretical estimates.

The three potentials examined so far are given as functions of Gaussians and thus depend on r_{ij}^2 . As is well known, in such a case the convergence of the HH expansion as a function of the grand angular quantum number is exponential and fast. We actually observe such a behavior in all three cases. However, especially for the class C1, the convergence is relatively more difficult for the two models with a repulsive core than in the Volkov case, confirming that the short-range repulsion is mostly responsible for the need of the two-body correlations.

The next examples considered are the MT-V and MT-I/III potentials. They are given as a superposition of Yukawians and

have a strong repulsive core with a $1/r$ divergence. As already mentioned they represent the most challenging problem for the HH expansion, due to the difficulty of constructing accurate two-body correlations at short interparticle distances, where the cancellation between kinetic and potential energy is critical. As can be seen by inspecting Table VI, the BE for the MT-V is slightly underestimated. We have already discussed this case in the previous subsection and we have seen that it is possible to obtain very precise estimates for the "missing" BE using the known behavior $\Delta \propto 1/K^5$. Adding this "missing" BE to the value $B = 31.347 \text{ MeV}$ brings the HH result very close to the estimates computed by other techniques. For the (S -wave) MT-I/III we observe that our estimate is already close to the very precise calculation of Ref. [22]. The "missing" BE in this case is estimated to be 21 keV, bringing our estimated BE to be 30.331 MeV.

Let us now consider the calculations performed using the realistic models of the NN interactions (see Table VII). Again the value $\hbar^2/m = 41.47108 \text{ MeV fm}^2$, corresponding to $2/m = 1/m_p + 1/m_n$, has been used. Let us consider first the calculations performed without any $3N$ interaction. We have considered here the AV18 and the Nijmegen II [6] (Nijm-II) interactions models. Both potentials belong to the group of the modern NN potentials which reproduce the NN Nijmegen data set [67] with a χ^2 per datum ≈ 1 . They have been selected because they are local in coordinate space, whereas other modern potentials either have a "nonlocal" term like ∇^2 (Nijmegen I potential [6]) or are given in momentum space (Bonn interaction [7]). Note that our technique does not, in principle, present any difficulties in treating these other kind of potentials. The only problem is that now it is not possible to solve the hyperradial second order differential equations by the method proposed in Ref. [56]. Work is in progress to overcome this difficulty and to compute the $A = 3$ and 4 WF's also with nonlocal potentials in coordinate or momentum space.

The convergence of the HH expansion in the case of the AV18 potential has been already discussed in the previous subsection. An analogous pattern of convergence is also found for the Nijm-II potential. In Table VII, the results for the BE and other properties are compared with the results of other techniques. Note that in the Nijm-II model we have included also the electromagnetic interactions, in addition to the Coulomb potential, as in the case of the AV18 potential. These terms contribute an additional -0.07 MeV to the BE and this explains the difference with the reported FY calculation, where they were not included. By taking into account this fact, our Nijm-II BE agrees well with the corresponding value obtained using the FY equations. Moreover, by taking into account the "missing" BE estimated as explained previously, our results practically reproduce the FY ones, by again taking into account the quoted 50-keV uncertainty of the latter method [24].

We now consider the inclusion of the $3N$ interaction. We have considered here two models: the already-discussed UIX and Tucson-Melbourne [13] (TM) models. In the latter case, we have used the modified version TM' , more consistent with chiral symmetry [68], with the cutoff parameter fixed to be $\Lambda = 4.756 m_\pi$ [3]. We have used them together with the AV18 potential (AV18+UIX and AV18+ TM' models). The cutoff

TABLE VIII. Percentages of the total isospin components $T = 1$ and 2 in the α -particle ground states for various interaction models.

Interaction	Method	$P_{T=1}$ (%)	$P_{T=2}$ (%)
AV18	HH this work	2.8×10^{-3}	5.2×10^{-3}
AV18	FY [24]	3×10^{-3}	5×10^{-3}
Nijm-II	HH this work	1.6×10^{-3}	7.4×10^{-3}
AV18+UIX	HH this work	2.5×10^{-4}	5.0×10^{-3}

parameter of the TM' $3N$ interaction was chosen to reproduce the BE of ${}^3\text{He}$. The inclusion of the UIX or the TM' models of the $3N$ interaction does not change the convergence behavior of the HH expansion and also in these cases it is possible to obtain nearly converged results (they have been obtained in the approximation described in Sec. IV D). Note that in the AV18+UIX case, the HH and FY estimates for the BE are slightly above the GFMC result. This is probably due to fact that in the GFMC technique, the L^2 and $(L \cdot S)^2$ terms of the NN interaction are not treated exactly and therefore the GFMC estimates have to be regarded as an upper bound of the true ground state energy.

In summary, the HH expansion has proved to be flexible enough to describe accurately the α -particle bound state using realistic NN and $3N$ interaction models.

C. Origin of the $T > 0$ components

In the calculations performed with the realistic NN and $NN + 3N$ interaction we have included components with total isospin $T = 0, 1$, and 2 in the WF. The calculated percentages of the states with $T = 1$ and 2 for the AV18 and AV18+UIX models are reported in Table VIII. The results obtained by the FY calculations [24] have been also reported. These components appear in the WF when the class C6 is included in the expansion. From Table IV, it can be seen that the convergence of the BE for that class is reached without difficulties, including states up to $K = 16$. However, the percentage values of the $T = 1$ and 2 states have been found to converge substantially more slowly and HH functions of class C6 up to $K = 32$ have to be considered. The contribution to the BE of the C6 states with $K > 16$ is very small, less than 1 keV.

As can be seen by inspecting Table VIII, the percentages of the components with $T = 1$ and 2 in the α -particle wave function are extremely small. For the AV18 potential, they are in good agreement with the FY estimates [24]. The percentages obtained using the Nijm-II potential differ by about 40% with respect to those obtained with the AV18. The inclusion of the $3N$ interaction tends to reduce them slightly. The adopted models of $3N$ interaction contain no isospin mixing term.

The knowledge of the $T = 1$ and 2 percentages is important for parity-violating experiments of electron scattering on ${}^4\text{He}$, devoted to studying the admixture of strange quark $s\bar{s}$ pairs in the nucleon. Information on this quantity can be extracted from the measurement of the "left-right" asymmetry A_{LR} of polarized electrons on a target nucleus, resulting from the interference between the electromagnetic and the weak neutral

current mediating the scattering process. The study of the asymmetry is particularly simple in case of a $(J^\pi, T) = (0^+, 0)$ system, because in that case the number of matrix elements entering this observable is small. Moreover, the use of ${}^4\text{He}$ as a target nucleus is also favored by the fact that its first excited state is at 20.1 MeV, which allows for an easy experimental control of inelastic processes. Indeed, there are approved experiments at the Jefferson Lab [69,70].

However, the extraction of the information from the experiments could be complicated by the presence of components with isospin $T = 1$ and 2 in the WF of ${}^4\text{He}$. This question was analyzed in Ref. [71] and found that the contribution from the $T = 1$ isospin mixing configurations to A_{LR} was negligible. Considering the effect of the Coulomb potential alone, the percentage of the $T = 1$ component in that work was estimated to be $P_{T=1} = 7 \times 10^{-4}$. From the present calculation, in agreement with the study of Ref. [24], the $T = 1$ component results to be 4 times larger and this could be of some effect on A_{LR} .

The presence of $T = 1$ and 2 components in the α -particle WF could play an important role also in the study of the reaction $d + d \rightarrow \alpha + \pi^0$. This reaction is possible only if the isospin symmetry is violated, namely it probes directly the charge symmetry breaking (CSB) terms in the nuclear Hamiltonian. These terms come from both the u - and d -quark mass difference (a fundamental quantity poorly known) and from electromagnetic effects. Very recently, such a reaction has been actually observed at IUCF [72], with a cross section at threshold ($E_d = 228.5$ MeV) of $\sigma = 12.7 \pm 2.2$ pb. Clearly, this reaction can take place since the α -particle WF has a nonvanishing $T = 1$ component. It can also proceed via some explicit CSB transition operators. The theoretical study of this reaction is currently under way [73].

Therefore, it is interesting to study the origin of the $T = 1$ and 2 isospin admixtures to the α -particle WF. To this end we have performed a series of calculations by removing from the Hamiltonian the different terms that induce the $T > 0$ components. Let us write the following:

$$H = H_{IC} + H_C + H_{CSB} + H_{e.m.} + K_\Delta, \quad (36)$$

where H_{IC} is the isospin-conserving part of the nuclear Hamiltonian, H_C the point-Coulomb interaction, H_{CSB} the charge symmetry breaking nuclear interaction (namely the operators 15–18 in AV18), $H_{e.m.}$ the remaining electromagnetic (e.m.) interaction (finite-size effects, vacuum polarization, magnetic moment interactions, etc.), and K_Δ the term originating from the proton and neutron mass difference in the kinetic energy. This latter term has not been included in the solution of the four-body problem and its effects have been evaluated perturbatively as explained in Appendix B.

By approximating the Hamiltonian with H_{IC} only, one would get no isospin admixture at all. We have then added the various terms one by one to H_{IC} and reported the results in Table IX. As can be seen from that table, with the inclusion of the Coulomb potential H_C , the percentage of the $T = 1$ state is in rough agreement (within a factor 2) with that estimated in Ref. [71]. The percentage of the $T = 2$ state is very tiny in this case. This can be understood from the perturbative treatment described in Appendix B.

TABLE IX. Effect of the inclusion of the various isospin mixing terms in the nuclear Hamiltonian on the percentages of the total isospin components $T = 1$ and 2 in the α -particle ground states. The calculations have been performed using the AV18 model for the nuclear Hamiltonian. For the explanation of the various terms H_{IC} , and so on, see the text.

Interaction	$P_{T=1}$ [%]	$P_{T=2}$ [%]
H_{IC}	0	0
$H_{IC} + H_C$	1.5×10^{-3}	0.1×10^{-3}
$H_{IC} + H_C + H_{CSB}$	3.0×10^{-3}	4.9×10^{-3}
$H_{IC} + H_C + H_{CSB} + H_{em}$	2.8×10^{-3}	5.2×10^{-3}

When the CSB terms of the AV18 NN interaction are taken into account, however, the previous picture is noticeably modified and both components increase, in particular the $T = 2$ component, which becomes larger than the $T = 1$ one. The CSB part of the AV18 potential is explicitly given by the following:

$$H_{CSB} = H_{I,CSB}^{(1)} + H_{I,CSB}^{(2)}, \quad (37)$$

$$H_{I,CSB}^{(1)} = \sum_{i < j} V^{(1)}(i, j) [\tau_z(i) + \tau_z(j)], \quad (38)$$

$$H_{I,CSB}^{(2)} = \sum_{i < j} V^{(2)}(i, j) \left[\tau_z(i)\tau_z(j) - \frac{1}{3} \boldsymbol{\tau}_i \cdot \boldsymbol{\tau}_j \right], \quad (39)$$

where $V^{(1)}(i, j)$ and $V^{(2)}(i, j)$ are functions depending on the interparticle distance r_{ij} and on the spin operators of the particles i and j . The operator $[\tau_z(i)\tau_z(j) - \frac{1}{3} \boldsymbol{\tau}_i \cdot \boldsymbol{\tau}_j]$ in $H_{I,CSB}^{(2)}$ induces differences between the pp and pn interactions (it originates mainly from the difference between the charged and neutral pion masses). These differences are well established and, although rather small, are of sizable value in some observables (such as the singlet np and pp scattering lengths). The operator $[\tau_z(i) + \tau_z(j)]$ in $H_{I,CSB}^{(1)}$ induces instead differences between the pp and nn interaction, too. Because of the lack of precise nn data, the magnitude of this charge independence breaking term is not very well known; however, its strength should satisfy $H_{I,CSB}^{(1)} \ll H_{I,CSB}^{(2)}$. The part $H_{I,CSB}^{(2)}$ is therefore responsible for the (relatively) large $T = 2$ state percentage in the α -particle ground-state WF. Finally, the effect of $H_{e.m.}$ is rather tiny as can be seen by inspecting Table IX (see also Appendix B).

Finally, in Appendix B, we have considered the effect of K_Δ on $P_{T=1,2}$, which has been found to be very small. The corresponding change in the α -particle BE is found to be $\delta B = +0.15$ keV. We can conclude that the effect of the $n - p$ mass difference to the BE and structure of the α particle is practically negligible.

D. Truncation studies

In prevision of future applications of the present technique to heavier systems, we have explored the effect of truncating part of the NN and $3N$ interaction. The aim is to find a way of simplifying the Hamiltonian, still obtaining very precise results, with a maximum deviation of the order of 0.1% with

TABLE X. Effects of the truncation of the NN potential when acting only on pairs having total angular momentum $j \leq j_M$ on the binding energy B (MeV), the expectation value of the kinetic energy operator $\langle K \rangle$ (MeV), and the P and D probabilities (%). The potential model chosen is the AV18 and the selected HH basis has $\{K_1, K_2, K_3, K_4, K_5, K_6\} = \{64, 40, 34, 24, 0, 0\}$.

j_M	B	$\langle K \rangle$	P_P	P_D
4	24.124	97.692	0.344	13.713
6	24.161	97.771	0.345	13.724
8	24.164	97.773	0.345	13.725
10	24.165	97.773	0.345	13.725
20	24.163	97.774	0.345	13.720
∞	24.163	97.774	0.345	13.720

respect to the results obtained with no approximation. We have explored both the effect of neglecting the NN interaction when the total angular momentum j of the pair is greater than a given value j_M and the effect of neglecting the $3N$ interaction when it acts on HH states with grand angular quantum number greater than a given K_M .

Let us first discuss the case of truncation of the NN interaction. We have considered an NN interaction that vanishes when acting on pairs with total angular momentum $j > j_M$ and have varied j_M to see the effect on the α -particle BE. We have considered the AV18 interaction, because its operatorial form allows one to compute it for arbitrary values of j . The results obtained can be seen in Table X. The calculation with $j_M = \infty$ means that we have retained the NN interaction acting in all states. By inspecting the table, it can be seen that by taking $j_M \geq 6$ the BE and other quantities vary very little. Therefore, it seems safe to retain the NN interaction as acting only on states with $j \leq 6 \div 8$.

Let us now consider the $3N$ interaction. The behavior of the radial parts of the UIX or TM' $3N$ potential are rather soft at short interparticle distances. Because the large grand angular quantum number components in the WF are induced by the repulsive core of the potentials, this suggests that the correlations induced by the $3N$ interaction would not need such high components. Therefore, we have included in the Hamiltonian an effective $3N$ interaction of the following kind:

$$\tilde{W}_{K_M}(i, j, k) = P_{K_M}^\dagger W(i, j, k) P_{K_M}, \quad (40)$$

where $W(i, j, k)$ is a $3N$ interaction and P_{K_M} a projection operator which gives 0 when it acts on four-body HH states with a given grand angular quantum number K having $K > K_M$. Actually, $\tilde{W}_{K_M}(i, j, k)$ is an effective four-body interaction. We have then studied the effects on the α -particle BE by varying K_M . We have considered here the AV18+UIX model. The results obtained can be found in Table XI, where for simplicity we have restricted the HH basis to include only the first three classes (in any case, the other classes include HH states with $K < 30$). As can be seen by inspecting the table, the BE and the other quantities depend very little on K_M . Already for $K_M = 20$, the corresponding BE differs from that obtained in the nontruncated case by less than 0.1%. The calculation of the $3N$ potential matrix elements between states with $K \leq 20 \div 30$ is noticeably simpler than in the general case

TABLE XI. Effects of the truncation of the $3N$ potential when acting only on four-body HH states of grand angular quantum number $K \leq K_M$ on the binding energy B (MeV), the expectation value of the kinetic energy operator $\langle K \rangle$ (MeV), and the P and D probabilities (%). The potential model chosen is the AV18+UIX and the selected HH basis has $\{K_1, K_2, K_3, K_4, K_5, K_6\} = \{64, 40, 34, 0, 0, 0\}$.

K_M	B	$\langle K \rangle$	P_P	P_D
20	27.351	109.71	0.596	15.05
24	27.366	109.67	0.596	15.05
30	27.372	109.65	0.596	15.05
34	27.374	109.64	0.596	15.05

and still the results are of acceptable precision. This should allow for HH calculations including $3N$ interactions also for scattering states and for heavier systems. This conclusion is also supported by the study of Ref. [74] of the incorporation of the $3N$ interaction in the EIH method. Note that the results reported in Tables IV and VII have been obtained using the $3N$ interactions “truncated” as in Eq. (40) and taking $K_M = 30$.

E. Asymptotic normalization constants

The asymptotic normalization constants (ANCs) are properties of the bound-state WF that can be related to experimental observables. They are interesting quantities from which useful information on the nuclear structure can be extracted. In particular, the D -state component percentage of the α particle can be revealed by a (d, α) reaction initiated by a tensor-polarized deuteron beam. In fact, an analysis of the experimental results can allow for the extraction of the “distorted-wave” parameter D_2^{dd} , in turn closely related to the asymptotic d - to s -state d - d ANCs ratio [75–78]. An estimate of D_2^{dd} using some of the modern $NN + 3N$ interactions are given below. The ANCs also provide a test of the quality of the variational WF in the asymptotic region, as we shall see. This test will be particularly severe in our approach, as the description of the ^4He WF in terms of the four-body HH functions in regions where the $1+3$ or $2+2$ clustering configurations are dominant will be difficult.

Let us concentrate first on the proton-triton ANC C_S^{pt} of ^4He , defined by the following:

$$\Psi_4(\xi_1, \xi_2, \xi_3) \rightarrow C_S^{pt} \sqrt{2\beta_{pt}} \frac{W_{-\eta_{pt}, 1/2}(2\beta_{pt} r_{pt})}{r_{pt}} \times \Phi_0^{pt}(\widehat{\xi}_1, \xi_2, \xi_3), \quad r_{pt} \rightarrow \infty, \quad (41)$$

where the Jacobi vectors ξ_i correspond to the permutation $p = 1$ (the index p will be suppressed in this section) and $r_{pt} = \sqrt{2/3} \xi_1$ is the distance between the ^3H center of mass and the fourth nucleon. The function Φ_L^{pt} is defined as follows:

$$\Phi_L^{pt}(\widehat{\xi}_1, \xi_2, \xi_3) = \{Y_L(\widehat{\xi}_1)[\psi_t(1, 2, 3)\chi_4\xi_4]_S\}_{0,0}, \quad (42)$$

where $\psi_t(1, 2, 3) \equiv \psi_t(\xi_2, \xi_3)$ is the ^3H WF and $\chi_4(\xi_4)$ is the spin (isospin) function of the fourth nucleon. In the previous equation, the spin $1/2$ of ^3H is coupled to the spin $1/2$ of the other nucleon to give a “channel” spin $S = 0, 1$. The channel

spin is in turn coupled to L to give a total angular momentum $J = 0$; therefore $L = S$. Because of the even parity of the ^4He state, the p - ^3H clusters can only be in the state $S = L = 0$. In Eq. (41), $W_{-\eta, j}(2\beta r)$ is the Whittaker function that behaves irregularly at the origin and decays exponentially for $r \rightarrow \infty$, whereas β_{pt} and η_{pt} are determined by the following:

$$\beta_{pt} = \sqrt{\frac{3m}{2\hbar^2}(B_4 - B_t)}, \quad \eta_{pt} = \frac{3m}{4\hbar^2} \frac{e^2}{\beta_{pt}}, \quad (43)$$

where $e^2 \approx 1.44$ MeV fm; $\hbar^2/m \approx 41.47$ MeV fm² and B_4 and B_t are the ^4He and ^3H BE, respectively. Finally, the factor $\sqrt{2\beta_{pt}}$ in Eq. (41) has been introduced so that the ANC C_S^{pt} is dimensionless.

To calculate C_S^{pt} , let us introduce the ^3H - ^4He overlap function as follows:

$$f_{pt}(r_{pt}) = \int d^3\xi_1 d^3\xi_2 d^3\xi_3 \delta\left(\sqrt{\frac{2}{3}}\xi_1 - r_{pt}\right) \times \frac{\Phi_0^{pt}(\widehat{\xi}_1, \xi_2, \xi_3)^\dagger}{r_{pt}} \Psi_4(\xi_1, \xi_2, \xi_3), \quad (44)$$

and the ratio

$$c_{pt}(r_{pt}) = \frac{f_{pt}(r_{pt})}{(3/2)^{\frac{3}{2}} \sqrt{2\beta_{pt}} W_{-\eta_{pt}, 1/2}(2\beta_{pt} r_{pt})}. \quad (45)$$

If Ψ_4 is the exact ^4He WF, for $r_{pt} \rightarrow \infty$ the overlap function behaves as follows:

$$f_{pt}(r_{pt}) \rightarrow \left(\frac{3}{2}\right)^{\frac{3}{2}} C_S^{pt} \sqrt{2\beta_{pt}} W_{-\eta_{pt}, 1/2}(2\beta_{pt} r_{pt}), \quad (46)$$

and therefore $c_{pt}(r_{pt}) \rightarrow C_S^{pt}$, allowing for the extraction of the ANC. The ^3H WF has been determined by means of the pair-correlated HH (PHH) technique described in Ref. [35] and is believed to be very precise [79]. The dependence to the truncation level of the HH basis used to compute the ^4He WF has been studied by computing the overlap function for the following three different choices of the maximum values of the grand angular quantum numbers of the six classes as defined in Sec. IVA as follows:

$$\begin{aligned} &\{K_{1M}, K_{2M}, K_{3M}, K_{4M}, K_{5M}, K_{6M}\} \\ &= \{56, 32, 26, 16, 14, 24\}, \quad \text{case a,} \\ &\{K_{1M}, K_{2M}, K_{3M}, K_{4M}, K_{5M}, K_{6M}\} \\ &= \{60, 36, 30, 20, 18, 28\}, \quad \text{case b,} \\ &\{K_{1M}, K_{2M}, K_{3M}, K_{4M}, K_{5M}, K_{6M}\} \\ &= \{64, 40, 34, 24, 22, 32\}, \quad \text{case c.} \end{aligned} \quad (47)$$

The corresponding ratios c_{pt} are shown in Fig. 3 by the open circles (case a), open squares, (case b) and solid triangles (case c). The potential used to generate the WF is the AV18 interaction. As can be seen by inspection of the figure, all three functions c_{pt} start to deviate from the expected asymptotic constant behavior already for $r_{pt} > 5$ fm, showing the difficulty of reproducing the cluster structure of the WF by means of the four-body HH functions. From the differences between the three ratios, the very slow convergence of $c_{pt}(r)$ as a function of $\{K_{1M}, K_{2M}, K_{3M}, K_{4M}, K_{5M}, K_{6M}\}$ results to

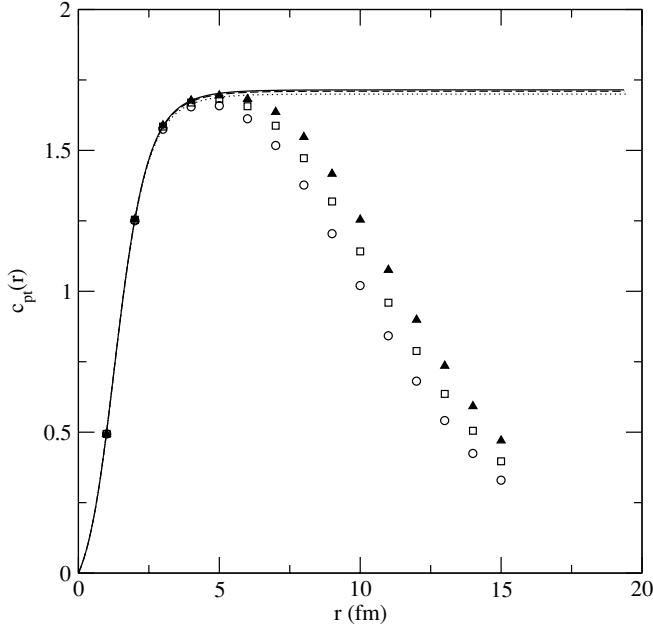


FIG. 3. Ratios $c_{pt}(r_{pt})$ as function of the p - ^3H distance r_{pt} . The ratios obtained by the direct calculation of the overlap using Eqs. (44) and (45) with the ^4He WF corresponding to the grand angular quantum numbers specified in Eq. (47) are shown by the open circles (case a), the open squares (case b), and the solid triangles (case c). The ratios obtained by the solution of the differential equation defined in Eq. (48) are shown by the dotted (case a), dashed (case b), and solid lines (case c), respectively (the dashed and solid line are almost coincident). The ^4He WF were generated using the AV18 potential.

be evident. In particular, a detailed analysis has shown that the convergence is sensitive to the value of K_{1M} . The ratio $c_{pt}(r)$ obtained with the larger basis shows a slightly larger “plateau” around $r_{pt} = 5$ fm, allowing for a crude estimate of the ANC, $C_S^{pt} \approx 1.7$.

To obtain a greater accuracy in the extraction of the ANC we have followed another procedure [80]. Assuming that Ψ_4 and ψ_t are “exact,” it is not difficult to show that the overlap function should satisfy the following differential equation:

$$-\frac{2\hbar^2}{3m} f_{pt}''(r) + \frac{e^2}{r} f_{pt}(r) + (B_4 - B_t) f_{pt}(r) + g(r) = 0, \quad (48)$$

where $r \equiv r_{pt}$ and

$$g(r) = \int d^3\xi_1 d^3\xi_2 d^3\xi_3 \delta\left(\sqrt{\frac{2}{3}}\xi_1 - r\right) \frac{\Phi_0^{pt}(\widehat{\xi}_1, \xi_2, \xi_3)^\dagger}{r} \times \left[V_{14} + V_{24} + V_{34} + W_{124} + W_{134} + W_{234} - \frac{e^2}{r} \right] \times \Psi_4(\xi_1, \xi_2, \xi_3), \quad (49)$$

V_{ij} and W_{ijk} being the NN and $3N$ potential, respectively. As $r \rightarrow \infty$, the function $g(r) \rightarrow 0$, and the solution of Eq. (48) coincides with the Whittaker function, allowing for the extraction of the ANC via Eq. (45). We have computed the function $g(r)$ with the three different choices of the ^4He

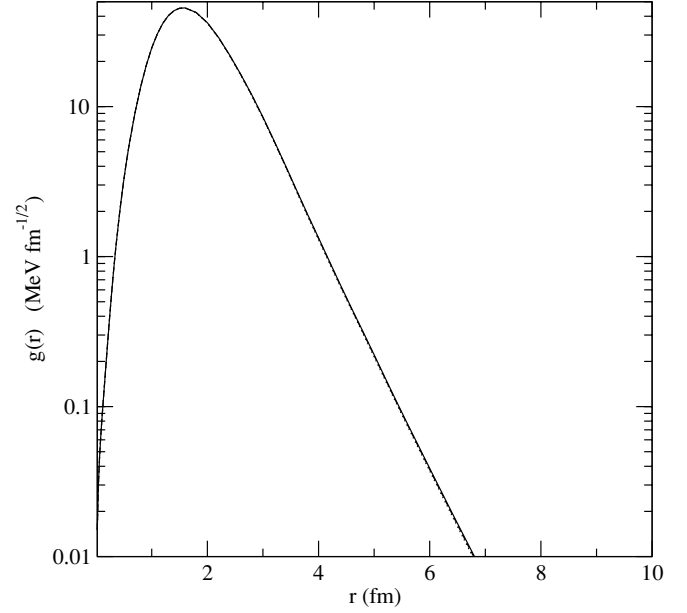


FIG. 4. Functions $g(r)$ obtained for three choices of the HH basis specified in Eq. (47) are shown by the dotted (case a), dashed (case b), and solid lines (case c). The three lines are practically coincident and cannot be distinguished.

WF Ψ_4 given in Eq. (47) and reported the results in Fig. 4. As can be seen, the function $g(r)$ is peaked at $r \approx 2$ fm, goes to zero exponentially, and depends slightly on the choice of Ψ_4 . In fact, the selected HH bases are already large enough to accurately describe the p - ^3H decomposition for $r < 4$ fm. For larger distances, probably $g(r)$ is not computed accurately using our variational WF, but there $g(r)$ becomes vanishingly small and the resulting effect on the ANC is negligible. This has been checked explicitly by solving Eq. (48) [imposing the boundary conditions $f_{pt}(0) = f_{pt}(\infty) = 0$] and computing $c_{pt}(r)$ for the same three cases as before. The results for $c_{pt}(r)$ are shown in Fig. 3 by the dotted, dashed, and solid lines (the results of the latter two cases are practically indistinguishable). As expected, for $r < 5$ fm, the line goes through the ratio functions $c_{pt}(r)$ computed directly via the overlap integral and reaches a constant value, corresponding to C_S^{pt} , around $r = 5$ fm. The extraction of the ANC can be now achieved with no difficulty and the value found is $C_S^{pt} = 1.715$.

An analogous procedure has been repeated for the n - ^3He ANC and the S - and D -wave d - d ANCs. We have used the following definition:

$$\Psi_4 \rightarrow C_S^{nh} \sqrt{2\beta_{nh}} \frac{e^{-\beta_{nh}r_{nh}}}{r_{nh}} \Phi_0^{nh}(\widehat{\xi}_1, \xi_2, \xi_3), \quad (50)$$

$$r_{nh} = \sqrt{\frac{2}{3}}\xi_1 \rightarrow \infty,$$

$$\Psi_4 \rightarrow C_S^{dd} \sqrt{2\beta_{dd}} \frac{W_{-n_{dd}, 1/2}(2\beta_{dd}r_{dd})}{r_{dd}} \Phi_0^{dd}(\xi'_1, \widehat{\xi}'_2, \xi'_3) + C_D^{dd} \sqrt{2\beta_{dd}} \frac{W_{-n_{dd}, 5/2}(2\beta_{dd}r_{dd})}{r_{dd}} \Phi_2^{dd}(\xi'_1, \widehat{\xi}'_2, \xi'_3), \quad (51)$$

TABLE XII. ANCs and the parameter D_2^{dd} obtained with the HH expansion and the solution of the differential equation of Eq. (48) for two potential models. The D_2^{dd} parameter is defined in Eq. (56). In the third row, the theoretical estimate for D_2^{dd} of Ref. [81] is also shown. Finally, in the last three rows, some available experimental values for the parameter D_2^{dd} have been also reported.

Parameter	C_S^{pt}	C_S^{nh}	C_S^{dd}	C_D^{dd}	D_2^{dd} (fm ²)
AV18	1.72	1.67	1.96	-0.209	-0.115
AV18+UIX	1.75	1.69	1.99	-0.277	-0.113
Adhikari <i>et al.</i> [81]					-0.12
Karp <i>et al.</i> [77]					-0.3 \pm 0.1
Merz <i>et al.</i> [82]					-0.19 \pm 0.04
Weller <i>et al.</i> [78]					-0.2 \pm 0.05

$$r_{dd} = \sqrt{\frac{1}{2}\xi_2'} \rightarrow \infty, \quad (52)$$

where ξ_i' are the set B of the Jacobi vectors defined in Eq. (29) corresponding to the permutation $p = 1$ and

$$\Phi_L^{nh}(\widehat{\xi}_1, \widehat{\xi}_2, \widehat{\xi}_3) = \{Y_L(\widehat{\xi}_1)[\psi_h(1, 2, 3)\chi_4\xi_4]_S\}_{0,0}, \quad (53)$$

$$\Phi_L^{dd}(\widehat{\xi}_1', \widehat{\xi}_2', \widehat{\xi}_3') = \{Y_L(\widehat{\xi}_2')[\phi_d(1, 2)\phi_d(3, 4)]_S\}_{0,0}. \quad (54)$$

In the latter, ψ_h and ϕ_d are the ^3He and deuteron WF, respectively, and

$$\beta_{nh} = \sqrt{\frac{3m}{2\hbar^2}(B_4 - B_h)}, \quad \beta_{dd} = \sqrt{\frac{2m}{\hbar^2}(B_4 - 2B_d)},$$

$$\eta_{dd} = \frac{m}{\hbar^2} \frac{e^2}{\beta_{dd}}, \quad (55)$$

with B_h and B_d the ^3He and deuteron BE, respectively. For the d - d case, one can also estimate the distorted-wave parameter D_2^{dd} defined by the following:

$$D_2^{dd} = \frac{1}{15} \int_0^\infty dr_{dd} r_{dd}^3 f_{dd}^D(r_{dd}) / \int_0^\infty dr_{dd} r_{dd} f_{dd}^S(r_{dd}), \quad (56)$$

where $f_{dd}^X(r_{dd})$ ($X = S, D$) are the S - and D -wave (d - d)⁴He overlap functions, respectively, defined in analogy to Eq. (44). The results obtained have been reported in Table XII, together with some other theoretical and experimental estimates available for D_2^{dd} (for a more complete list of references, see Ref. [81]). The D_2^{dd} parameter was determined in Ref. [81] using an approximated method (a cluster model) which however seems to provide an estimate rather close to ours. This parameter is also in reasonable agreement with the experimental values reported in Table XII, also considering the difficulty of the extraction of this quantity from the experimental data.

F. Details of the practical implementation of the method

It may be opportune at this point to give some detail of the computer resources needed to perform the full calculation. The first step consists of computing the transformations coefficients given in Eq. (23). This task can be performed once and for

all as it does not depend on the adopted potential model. The coefficients are then stored in computer disks (in the present case, they occupy about 4 Gb of disk space). The orthogonalization does not present a problem of CPU time, as it can be separately performed for each subspace of HH functions of given K, L, S, T quantum numbers.

The second step is to compute the one-dimensional integrals of the NN potential given in Eq. (28). The CPU time depends noticeably by the value of j_M defined in the Sec. IV D. Taking $j_M \rightarrow \infty$, the calculation can last several hours, which are reduced to a few hours when $j_M = 10$ or less. Also these integrals can be saved on a computer disk (the allocated space in this case is less than 1 Gb).

The third step consists in the calculation of the NN potential matrix elements

$$\langle \Psi_\mu^{KLS TJ\pi} | V(1, 2) | \Psi_{\mu'}^{K'L'S'T'J\pi} \rangle. \quad (57)$$

This task is simply reduced to a sum of products of the transformation coefficients $B_{\mu,\nu}^{KLS TJ\pi}$, defined in Eq. (23), and the integrals given in Eq. (28) calculated as discussed above. The NN matrix elements (which are function of ρ) are again written in a computer disk. For example, in a calculation with 5000 HH functions, a grid of 65 points in ρ , and storing the matrix elements as double precision numbers, the needed disk space is about 6 Gb. Most of the CPU time here is spent in disk I/O and therefore the total time of this calculation depends critically on the particular computer used. For the case $j_M \rightarrow \infty$, using a “normal” pentium PC, where the I/O speed is not very high, the calculation can last several days. When $j_M = 10$ or less, the task is noticeably simplified, allowing the calculation to be performed in 1–2 days. Using a more sophisticated machine, this time could be reduced to less than 1 day.

In parallel, one can eventually calculate the matrix elements of a $3N$ interaction. As explained in Appendix A, again this task is divided in two steps: calculation of the integrals given in Eqs. (A10)–(A11) and the sum given in Eq. (A12). The first part can be performed beforehand and the values of $I_{i,j,k}^{p,q}$ and $J_{i,j,k}^{p,q}$ stored in computer disks (the CPU time and disk space needed in this case is rather small). To evaluate the sum given in Eq. (A12), one needs the integrals (A7). This part can be easily parallelized to run on a PC farm,

and so on. The CPU time depends very critically on the value of K_M used to “truncate” the $3N$ interaction as given in Eq. (40). Calculations with $K_M \geq 40$ appeared impossible with the computers available to the authors. Calculations with $K_M \approx 30$ are rather lengthy but possible (several days using 16 CPUs). Calculations with $K_M = 20$ are much less time consuming and still very accurate. The disk space used to store the $3N$ potential matrix elements is correspondingly very small for $K_M = 20$ (< 1 Gb), and it increases like K_M^2 .

The last step corresponds to the solution of the second-order differential equations for the functions $u_{KLS\mu}(\rho)$. Also in this case the I/O speed of the computer is the critical factor. The calculation corresponding to the full basis can take several hours of CPU time on a small computer.

In summary, having prepared beforehand the transformation coefficients and the integrals given in Eq. (28), a calculation with a NN potential can be performed in a few days. Including a $3N$ interaction with $K_M = 20$ would take a similar time, having the possibility to run the code on a (small) parallel machine.

V. CONCLUSIONS AND PERSPECTIVES

We have studied the solution of the Schroedinger equation for the four-nucleon ground state using the HH function expansion. The main difficulty when using the HH basis is its large degeneracy, accordingly a suitable selection of the HH functions giving the most important contributions has to be performed. In this work, the HH functions have been divided into classes, depending on the number of correlated particles, the values of the orbital angular momenta, the total isospin quantum number, and so on. For each class, the expansion has been truncated so as to obtain the required accuracy. We have applied this procedure in particular to the study of the ground state of the α particle using a number of NN and $NN + 3N$ interaction models. In all the cases, accurate calculations of the BE and other ground-state properties, such as the asymptotic normalization constants, have been achieved.

A similar procedure can be also applied for solving scattering problems. The calculation of the phase shifts and the various observables for n - ^3H and p - ^3He elastic scattering is now in progress and will be published elsewhere [83].

The hyperspherical formalism is adequate for treating all kinds of modern potentials, except those containing a hard core. We have considered here the AV18 and Nijmegen-II NN potentials and the UIX and TM' $3N$ interactions. The inclusion of the ∇^2 term present in the Nijmegen-I [6] potential introduces no additional difficulties. As an example, such a term was taken into account in Ref. [84] where the PHH approach was used. Moreover, the HH method can be easily formulated in momentum space. It can therefore be applied also to the case of the Bonn potential [7] although one additional numerical integration and the solution of an integral equation are then required. The application of the HH technique to the $A = 3, 4$ systems with the Bonn potential is actually underway.

At present there are only a few other methods available for accurate calculations of the four-nucleon problem, in particular taking into account a $3N$ force. There are two

other important motivations behind this work. The first one is to show in detail that the HH expansion applied to the four-nucleon bound and scattering problems is very powerful even for realistic NN interactions. The second motivation is the possibility of the extension of the method to larger systems. The feasibility of such an application would require the solution of the following different problems. First, the calculation of the generalized “Raynal-Revai” coefficients, namely of the coefficients relating HH functions constructed with different sets of Jacobi vectors. The direct generalization of the algorithm proposed in Ref. [55] is adequate for $A = 5 \div 8$. Otherwise, different algorithms could be used [52–54]. Second, the computation of the matrix elements of NN and $3N$ interactions, which can be reduced to the evaluation of low-dimensional integrals as in the present case. In particular, the possibility of approximating the $3N$ interaction as acting only on HH functions of low K , as discussed in Sec. IV D, should appreciably simplify this task. Finally, the choice of an optimal subset of HH functions. As A grows, the number of HH states for a given K increases very rapidly. The criteria for selecting the subclasses of HH functions chosen in the present article can be readily generalized to systems with $A > 4$. However, additional properties of the HH function could be exploited to further reduce the number of terms in the expansion. For example, one could take into account the symmetry of the space part of the states constructed as a product of the HH functions and the spin-isospin states. Another possibility to be explored is to include classes of HH functions constructed with those Jacobi vectors pertaining to different partitions of the particles. For example, in the study of the $d + ^3\text{H} \rightarrow ^4\text{He} + p$ reaction, the use of HH functions constructed in terms of $2 + 3$ and $4 + 1$ clusterizations should be very useful. Alternatively, one could try to integrate the present study with the effective interaction formalism [33,34].

ACKNOWLEDGMENTS

The authors thank Professor R. Schiavilla and Professor L. Lovitch for useful discussions and a critical reading of the manuscript.

APPENDIX A: THE MATRIX ELEMENTS OF A LOCAL $3N$ FORCE

In this Appendix, the method used for calculating the matrix elements of a local $3N$ interaction operator H_{3N} between the antisymmetric hyperangular-spin-isospin states defined in Eq. (11) will be briefly illustrated. The major problem to be overcome is to achieve a sufficient numerical precision, so that the differential equations for the functions $u_{KLS\mu}(\rho)$ defined in Eq. (22) could be solved without any numerical trouble. In general, a $3N$ interaction is written as follows:

$$H_{3N} = \sum_{i < j < k} \sum_{\text{cyclic}} W_{3N}(i; j, k), \quad (\text{A1})$$

where \sum_{cyclic} represents a cyclic sum over indices i, j , and k and $W_{3N}(i; j, k)$ is symmetric under the exchange of the

particles j and k . Therefore, the problem can be reduced to the computation of the matrix element of the operator $W_{3N}(1; 2, 3)$. Once the antisymmetric hyperangular-spin-isospin states are expanded in terms of the jj states as in Eq. (23), one has to compute the following integrals:

$$\mathcal{W}_{v,v'}(\rho) = \int d\Omega \langle \Xi_v^{KTJ\pi}(1, 2, 3, 4) | \times W_{3N}(1; 2, 3) | \Xi_{v'}^{K'TJ\pi}(1, 2, 3, 4) \rangle, \quad (\text{A2})$$

where the states $\Xi_v^{KTJ\pi}(1, 2, 3, 4)$ are defined in Eq. (24) (hereafter all the Jacobi vectors are chosen to correspond to the permutation $p = 1$, and therefore the index p will be omitted). In the case of the Urbana or TM-like $3N$ interactions, $W_{3N}(1; 2, 3)$ can be taken to have the following general form [85]:

$$W_{3N}(1; 2, 3) = \sum_{p,q=1}^6 F_{p,q}(r_{12}, r_{13}, \mu_{12,13}) \mathcal{O}_{12}^p \mathcal{O}_{13}^q, \quad (\text{A3})$$

where $\mu_{12,13} = \widehat{r}_{12} \cdot \widehat{r}_{13}$ and r_{ij} is the relative distance between the particles i and j . In the latter equation, $\mathcal{O}_{ij}^{p=1,6}$ are the following operators:

$$\mathcal{O}_{ij}^{p=1,6} = 1, (\boldsymbol{\tau}_i \cdot \boldsymbol{\tau}_j), (\boldsymbol{\sigma}_i \cdot \boldsymbol{\sigma}_j), (\boldsymbol{\sigma}_i \cdot \boldsymbol{\sigma}_j)(\boldsymbol{\tau}_i \cdot \boldsymbol{\tau}_j), r_{ij}^2 S_{ij}, r_{ij}^2 S_{ij}(\boldsymbol{\tau}_i \cdot \boldsymbol{\tau}_j), \quad (\text{A4})$$

where S_{ij} is the tensor operator (the factor r_{ij}^2 has been included in the definition of $\mathcal{O}^{p=5,6}$ so that these operators are polynomials in the Cartesian coordinates of the particles).

Because $W_{3N}(1; 2, 3)$ depends only on the variables $\rho, \varphi_3, \varphi_2, \widehat{\xi}_2, \widehat{\xi}_3$ we can easily integrate over the variables $\widehat{\xi}_1$. Moreover, by evaluating the spin-isospin traces and the integrals over the angles $\widehat{\xi}_2, \widehat{\xi}_3$ (except for $\mu = \widehat{\xi}_2 \cdot \widehat{\xi}_3$) one reduces the matrix element given in Eq. (A2), to an integral of the type:

$$\mathcal{W}_{v,v'}(\rho) = \sum_{p,q} \int_{-1}^1 dz \sqrt{1+z} \int_{-1}^1 dx \sqrt{1-x^2} \times \int_{-1}^1 d\mu F_{p,q}(r_{12}, r_{13}, \mu_{12,13}) \mathcal{P}_{p,q}(z, x, \mu) \quad (\text{A5})$$

where

$$z = \cos 2\varphi_3 = 2 \frac{r_{12}^2}{\rho^2} - 1, \quad x = \cos 2\varphi_2 = 2 \frac{\xi_2^2}{\rho^2} - 1, \quad (\text{A6})$$

and

$$\mathcal{P}_{p,q}(z, x, \mu) = \frac{(4\pi)^2}{128\sqrt{2}} \int d\widehat{\xi}_1 \langle \Xi_v^{KTJ\pi}(1, 2, 3, 4) | \times | \mathcal{O}_{12}^p \mathcal{O}_{13}^q | \Xi_{v'}^{K'TJ\pi}(1, 2, 3, 4) \rangle. \quad (\text{A7})$$

In Eq. (A7) the integration over the angles $\widehat{\xi}_2, \widehat{\xi}_3$ (except for $\mu = \widehat{\xi}_2 \cdot \widehat{\xi}_3$) and the trace over the spin-isospin degrees of freedom is implicit. This latter part of the calculation can be performed analytically in terms of Wigner D matrices and Clebsch-Gordan coefficients. The remaining two-dimensional integration over $d\widehat{\xi}_1 = d \cos \theta_1 d\phi_1$ in Eq. (A7) can be easily

performed by taking into account that the integrand is a polynomial in $\cos \theta_1$ and $\cos \phi_1$ of degree $K + K'$.

The functions \mathcal{P} can be therefore calculated *exactly* using an appropriate Gauss integration formula with a small number of points. Conversely, the functions $F_{p,q}$ entering the tridimensional integral (A5) are very complicated functions of the variables z, x, μ . Therefore, the integral (A5) requires the use of extended and dense integration grids [about $(1000)^3$ points] to yield the needed accuracy. Because the same integration has to be repeated for each v, v' , the complete calculation of $\mathcal{W}_{v,v'}$ could be very time consuming.

However, the function $\mathcal{P}_{p,q}(z, x, \mu)$ can be written in general as follows:

$$\mathcal{P}_{p,q}(z, x, \mu) = \mathcal{P}_{p,q}^e(z, x, \mu) + \sqrt{1+x} \sqrt{1-z^2} \mathcal{P}_{p,q}^o(z, x, \mu), \quad (\text{A8})$$

where $\mathcal{P}_{p,q}^e$ and $\mathcal{P}_{p,q}^o$ are polynomials in z, x , and μ of maximum degree $N = K + K' + 2$, the 2 coming (eventually) from the factor r_{ij}^2 multiplying the tensor operators in Eq. (A4). More precisely $\mathcal{P}^e(\sqrt{1+x}\sqrt{1-z^2}\mathcal{P}^o)$ is the even (odd) part of \mathcal{P} with respect to the variable μ .

Now, if $p(t)$ is a polynomial of degree n with respect to the variable t and its value in each of $n + 1$ points t_1, \dots, t_{n+1} is known, using the following ‘‘Lagrange interpolation’’ formula, $p(t)$ can be computed *exactly* for any t :

$$p(t) = \sum_{i=1, \dots, n+1} p(t_i) L_i^{(n+1)}(t), \quad (\text{A9})$$

$$L_i^{(n+1)}(t) \equiv \prod_{j=1, \dots, n+1, j \neq i} \frac{t - t_j}{t_i - t_j}.$$

Therefore, once three sets of points z_1, \dots, z_{N+1} , x_1, \dots, x_{N+1} , and μ_1, \dots, μ_{N+1} in the interval $(-1, 1)$ have been selected, and $\mathcal{P}_{p,q}^{e,o}$ in the $(N + 1)^3$ points z_i, x_j, μ_k have been computed, the functions $\mathcal{P}_{p,q}$ are then known *exactly* for all possible values of (z, x, μ) . Because the matrix elements of the $3N$ interaction are needed only between HH states with $K \lesssim 30$ (and therefore $\max[N] \ll 100$), as discussed in Sec. IV D, this means that in practice the functions \mathcal{P} have to be evaluated only a fairly small number of times. Finally, if we evaluate the following:

$$I_{i,j,k}^{p,q} = \int_{-1}^1 dz \sqrt{1+z} \int_{-1}^1 dx \sqrt{1-x^2} \times \int_{-1}^1 d\mu F_{p,q}(r_{12}, r_{13}, \mu_{12,13}) \times L_i^{(N+1)}(z) L_j^{(N+1)}(x) L_k^{(N+1)}(\mu), \quad (\text{A10})$$

$$J_{i,j,k}^{p,q} = \int_{-1}^1 dz \sqrt{1+z} \int_{-1}^1 dx \sqrt{1-x^2} \times \int_{-1}^1 d\mu F_{p,q}(r_{12}, r_{13}, \mu_{12,13}) \sqrt{1+x} \times \sqrt{1-z^2} L_i^{(N+1)}(z) L_j^{(N+1)}(x) L_k^{(N+1)}(\mu), \quad (\text{A11})$$

the required matrix elements can be obtained simply as follows:

$$\mathcal{W}_{\nu,\nu'}(\rho) = \sum_{p,q} \sum_{i,j,k=1}^N [\mathcal{P}_{p,q}^e(z_i, x_j, \mu_k) \times I_{i,j,k}^{p,q} + \mathcal{P}_{p,q}^o(z_i, x_j, \mu_k) J_{i,j,k}^{p,q}]. \quad (\text{A12})$$

where the integrals given in Eqs. (A10) and (A11) no longer depend on the quantum numbers ν, ν' of the HH states and therefore can be computed with the necessary accuracy once and for all and stored on computer disks. In this way, the matrix elements $\mathcal{W}_{\nu,\nu'}(\rho)$ obtained via Eq. (A12) are obtained very quickly [with only $\sim(N+1)^3$ operations].

APPENDIX B: THE $n-p$ MASS DIFFERENCE

To analyze the effect of $n-p$ mass difference, we have repeated the approximate calculation of Ref. [71]. Let us write the Hamiltonian of our system as in Eq. (36),

$$H = H_{IC} + H_C + H_{CSB} + H_{e.m.} + K_{\Delta} \equiv H^{(0)} + H_I^{(1)} + H_I^{(2)}, \quad (\text{B1})$$

namely as a sum of an isoscalar, isovector, and isotensor term. Let us treat $H^{(0)}$ as the unperturbed Hamiltonian and try to evaluate the $T > 0$ components using first-order perturbation theory. Namely

$$|\delta\Psi^{(T)}\rangle = \sum_{n>0} |\Psi_n\rangle \frac{\langle\Psi_n|H_I^{(T)}|\Psi_0\rangle}{E_0 - E_n}, \quad (\text{B2})$$

where Ψ_0 is the unperturbed ground state and $\Psi_n, n = 1, 2, \dots$ the unperturbed excited states of $H^{(0)}$, which therefore have definite values of the total isospin quantum number. In particular, Ψ_0 has $T = 0$, and so on. The most important contributions to the components $T = 1, 2$ of $\delta\Psi^{(T)}$ would come from the lowest excited states. Following Ref. [71] (see also Ref. [86]), we model these states as follows:

$$|\Psi_1^{(T)}\rangle = \frac{\Omega_T |\Psi_0\rangle}{\langle\Psi_0|\Omega_T^\dagger \Omega_T |\Psi_0\rangle^{1/2}}, \quad (\text{B3})$$

where $\Omega_T, T = 1, 2$, are excitation operators of the form

$$\Omega_1 = \sum_{ij} r_{ij}^2 (\tau_z(i) + \tau_z(j)), \quad (\text{B4})$$

$$\Omega_2 = \sum_{ij} r_{ij}^2 (\tau_z(i)\tau_z(j) - (1/3)\boldsymbol{\tau}(i) \cdot \boldsymbol{\tau}(j)). \quad (\text{B5})$$

The operator Ω_1 generates a state $(J^\pi, T) = (0^+, 1)$ corresponding to a ‘‘breathing’’ mode where neutrons and protons oscillate in counterphase. Furthermore, Ω_2 generates a state $(J^\pi, T) = (0^+, 2)$ with ‘‘tensor’’ oscillations. The $T = 1, 2$ components in the ${}^4\text{He}$ wave function would be given by the following:

$$|\delta\Psi^{(T)}\rangle \approx |\Psi_1^{(T)}\rangle \frac{\langle\Psi_1^{(T)}|H_I^{(T)}|\Psi_0\rangle}{E_0 - E_1^{(T)}} \equiv \chi_T |\Psi_1^{(T)}\rangle, \quad (\text{B6})$$

where $E_1^{(T)} = \langle\Psi_1^{(T)}|H^{(0)}|\Psi_1^{(T)}\rangle$. The percentage of the T wave is just $100|\chi_T|^2$.

In the following, we applied the procedure outlined above using the AV18 potential model. Ψ_0 is the WF computed with the HH expansion excluding any states belonging to the class C6. We have found the following:

$$E_0 = -24.19 \text{ MeV}, \quad E_1^{(1)} = 7.05 \text{ MeV}, \quad E_1^{(2)} = 29.07 \text{ MeV}. \quad (\text{B7})$$

To check the consistency of this procedure, let us consider the (point) Coulomb potential H_C , given by the following:

$$H_C = \sum_{i<j} \frac{e^2}{r_{ij}} \left(\frac{1 + \tau_z(i)}{2} \right) \left(\frac{1 + \tau_z(j)}{2} \right) \quad (\text{B8})$$

and therefore the terms entering $H_I^{(1)}$ and $H_I^{(2)}$ are as follows:

$$H_{I,C}^{(1)} = \sum_{i<j} \frac{e^2}{r_{ij}} \left(\frac{\tau_z(i) + \tau_z(j)}{4} \right), \quad (\text{B9})$$

$$H_{I,C}^{(2)} = \sum_{i<j} \frac{e^2}{r_{ij}} \left(\frac{\tau_z(i)\tau_z(j) - \frac{1}{3}\boldsymbol{\tau}(i) \cdot \boldsymbol{\tau}(j)}{4} \right). \quad (\text{B10})$$

The necessary matrix elements can be readily computed with the result that

$$\begin{aligned} \langle\Psi_1^{(T=1)}|H_{I,C}^{(T=1)}|\Psi_0\rangle &\approx -100 \text{ keV}, \\ \langle\Psi_1^{(T=2)}|H_{I,C}^{(T=2)}|\Psi_0\rangle &\approx -37 \text{ keV}. \end{aligned} \quad (\text{B11})$$

and therefore $P_{T=1} \approx 1 \times 10^{-3}$ and $P_{T=2} \approx 0.05 \times 10^{-3}$ confirming that the $T = 2$ component induced by the Coulomb potential is smaller than the $T = 1$ one. In fact, the radial dependence (and strength) of $H_{I,C}^{(1)}$ and $H_{I,C}^{(2)}$ are the same. However, the $T = 2$ breathing mode has a higher excited energy and this reduces the probability of a ‘‘transition’’ to the state $|\Psi_1^{(T=2)}\rangle$. The values $P_{T=1}$ and $P_{T=2}$ are also in agreement within a factor 2 with the results reported in the second row of Table IX. Therefore, we expect that the estimate of the isospin admixture percentage using this approximate method are of the right order of magnitude.

Considering now the CSB interaction, we have found the following:

$$\begin{aligned} \langle\Psi_1^{(T=1)}|H_{I,CSB}^{(T=1)}|\Psi_0\rangle &\approx -23 \text{ keV}, \\ \langle\Psi_1^{(T=2)}|H_{I,CSB}^{(T=2)}|\Psi_0\rangle &\approx -84 \text{ keV}, \end{aligned} \quad (\text{B12})$$

where $H_{I,CSB}^{(T=1,2)}$ are defined in Eqs. (38) and (39). As expected, the matrix elements $\langle\Psi_1^{(T=2)}|H_{I,CSB}^{(T=2)}|\Psi_0\rangle$ are larger than the corresponding matrix elements of $H_{I,CSB}^{(1)}$. Adding the values given in Eqs. (B11) and (B12), we find $P_{T=1} = 1.5 \times 10^{-3}$ and $P_{T=2} = 0.6 \times 10^{-3}$ as the percentage of the isospin components induced by the Coulomb+CSB part of the Hamiltonian. Our approximate calculation seems to underestimate both component percentages (in particular $P_{T=2}$), but it is in qualitative agreement with the results reported in Table IX.

The e.m. part of the Hamiltonian produces small effects. This is also supported by our approximate calculation. We

have found, in fact, the following:

$$\langle \Psi_1^{(T=1)} | H_{e.m.} | \Psi_0 \rangle \approx 6 \text{ keV}, \quad \langle \Psi_1^{(T=2)} | H_{e.m.} | \Psi_0 \rangle \approx -3 \text{ keV}. \quad (\text{B13})$$

Let us finally apply the perturbative treatment to the mass difference between neutrons and protons. The associated term in the Hamiltonian is as follows:

$$K_\Delta = \sum_{i=1,4} \frac{1}{2} \left(\frac{1}{2m_p} - \frac{1}{2m_n} \right) \nabla_i^2 \tau_z(i) \equiv H_{I,\Delta}^{(1)}, \quad (\text{B14})$$

and therefore K_Δ is an isovector operator contributing to $H_I^{(1)}$ and may increase the percentage of the $T = 1$ state. We have found the following:

$$\langle \Psi_1^{(T=1)} | H_{I,\Delta}^{(1)} | \Psi_0 \rangle \approx -9 \text{ keV}. \quad (\text{B15})$$

The effect of K_Δ is therefore rather small as it would produce a change of $P_{T=1}$ of about 0.1×10^{-4} .

As a by-product of this calculation, we can also estimate the change in the BE produced by taking into account the

$n - p$ mass difference. First of all, let us restrict to the case $H = H^{(0)} + K_\Delta$ and let us treat K_Δ as a perturbation. Then, the first-order energy shift δE_1 vanishes, whereas the second order can be computed as outlined above to be as follows:

$$\delta E_2 \approx \frac{|\langle \Psi_1^{(T=1)} | K_\Delta | \Psi_0 \rangle|^2}{E_0 - E_1^{(T=1)}} \approx -0.003 \text{ keV}, \quad (\text{B16})$$

a very small change. However, one has to take into account the $T > 0$ components present in the α -particle wave function because of the Coulomb, CSB interaction, and so on. Therefore, we consider now $H_{IC} + H_C + H_{CSB} + H_{e.m.}$ as the unperturbed Hamiltonian and use the first order perturbation theory. As unperturbed WF we now use Ψ_{full} , namely that computed including in the expansion the HH components of all classes C1–C6. For the AV18 case, we find the following:

$$\langle \Psi_{\text{full}} | K_\Delta | \Psi_{\text{full}} \rangle = -0.15 \text{ keV}. \quad (\text{B17})$$

We can conclude that the effect of the $n - p$ mass difference to the BE and structure of the α particle is practically negligible.

-
- [1] H. Kamada *et al.*, Phys. Rev. C **64**, 044001 (2001).
[2] B. S. Pudliner, V. R. Pandharipande, J. Carlson, S. C. Pieper, and R. B. Wiringa, Phys. Rev. C **56**, 1720 (1997).
[3] A. Nogga, H. Kamada, and W. Glöckle, Phys. Rev. Lett. **85**, 944 (2000).
[4] R. B. Wiringa, S. C. Pieper, J. Carlson, and V. R. Pandharipande, Phys. Rev. C **62**, 014001 (2000).
[5] R. B. Wiringa, V. G. J. Stoks, and R. Schiavilla, Phys. Rev. C **51**, 38 (1995).
[6] V. G. J. Stoks, R. A. M. Klomp, C. P. F. Terheggen, and J. J. deSwart, Phys. Rev. C **49**, 2950 (1994).
[7] R. Machleidt, F. Sammarruca, and Y. Song, Phys. Rev. C **53**, R1483 (1996).
[8] R. Machleidt, Phys. Rev. C **63**, 024001 (2001).
[9] P. Doleschall and I. Borbély, Phys. Rev. C **62**, 054004 (2000).
[10] P. Doleschall, I. Borbely, Z. Papp, and W. Plessas, Phys. Rev. C **67**, 064005 (2003).
[11] R. Lazauskas and J. Carbonell, Phys. Rev. C **70**, 044002 (2004); see also arXiv:nucl-th/0408048.
[12] P. Navrátil and E. Caurier, Phys. Rev. C **69**, 014311 (2004).
[13] S. A. Coon *et al.*, Nucl. Phys. **A317**, 242 (1979).
[14] H. T. Coelho, T. K. Das, and M. R. Robilotta, Phys. Rev. C **28**, 1812 (1983).
[15] S. Weinberg, Phys. Lett. **B251**, 288 (1990).
[16] U. van Kolck, Phys. Rev. C **49**, 2932 (1994).
[17] E. Epelbaum, W. Glöckle, and Ulf-G. Meissner, Nucl. Phys. **A671**, 295 (2000); see also arXiv:nucl-th/0405048 and reference therein.
[18] D. R. Entem and R. Machleidt, Phys. Rev. C **68**, 041001(R) (2003).
[19] E. Epelbaum *et al.*, Phys. Rev. C **66**, 064001 (2002).
[20] O. Yakubovsky, Sov. J. Nucl. Phys. **5**, 937 (1967).
[21] H. Kamada and W. Glöckle, Nucl. Phys. **A548**, 205 (1992); W. Glöckle and H. Kamada, Phys. Rev. Lett. **71**, 971 (1993).
[22] N. W. Schellingerhout, J.J. Schut, and L. P. Kok, Phys. Rev. C **46**, 1192 (1992).
[23] F. Ciesielski, J. Carbonell, and C. Gignoux, Nucl. Phys. **A631**, 635c (1998); F. Ciesielski and J. Carbonell, Phys. Rev. C **58**, 58 (1998).
[24] A. Nogga, H. Kamada, W. Glöckle, and B. R. Barrett, Phys. Rev. C **65**, 054003 (2002).
[25] J. Carlson, Phys. Rev. C **38**, 1879 (1988).
[26] K. Varga and Y. Suzuki, Phys. Rev. C **52**, 2885 (1995).
[27] Y. Suzuki and K. Varga, *Stochastic Variational Approach to Quantum Mechanical Few-Body Problems* (Springer-Verlag, Berlin, 1998).
[28] H. Kameyama, M. Kamimura, and Y. Fukushima, Phys. Rev. C **40**, 974 (1989).
[29] M. Kamimura and H. Kameyama, Nucl. Phys. **A508**, 17c (1990).
[30] P. Navrátil and B. R. Barrett, Phys. Rev. C **59**, 1906 (1999).
[31] P. Navrátil, J. P. Vary, and B. R. Barrett, Phys. Rev. Lett. **84**, 5728 (2000); Phys. Rev. C **62**, 054311 (2000).
[32] P. Navrátil and W. E. Ormand, Phys. Rev. Lett. **88**, 152502 (2002).
[33] N. Barnea, W. Leidemann, G. Orlandini, Phys. Rev. C **61**, 054001 (2000).
[34] N. Barnea, W. Leidemann, and G. Orlandini, Phys. Rev. C **67**, 054003 (2003).
[35] A. Kievsky, S. Rosati, and M. Viviani, Nucl. Phys. **A577**, 511 (1994).
[36] M. Viviani, A. Kievsky, and S. Rosati, Nucl. Phys. **A737**, 205c (2004).
[37] A. C. Fonseca, Phys. Rev. Lett. **83**, 4021 (1999).
[38] M. Viviani, A. Kievsky, S. Rosati, E. A. George, and L. D. Knutson, Phys. Rev. Lett. **86**, 3739 (2001).
[39] B. Pfitzinger, H. M. Hofmann, and G. M. Hale, Phys. Rev. C **64**, 044003 (2001).
[40] M. Viviani, A. Kievsky, and S. Rosati, Few-Body Systems **18**, 25 (1995).
[41] M. Viviani, S. Rosati, and A. Kievsky, Phys. Rev. Lett. **81**, 1580 (1998).

- [42] V. F. Demin, Yu. E. Pokrovsky, and V.D. Efros, *Phys. Lett.* **B44**, 227 (1973).
- [43] B. A. Fomin and V. D. Efros, *Sov. J. Nucl. Phys.* **34**, 327 (1981); *Phys. Lett.* **B98**, 389 (1981).
- [44] J. L. Ballot, *Few-Body Systems Suppl.* **1**, edited by C. Ciofi degli Atti, O. Benhar, E. Pace, and G. Salmé (Springer-Verlag, Wien, 1987), p. 140.
- [45] J. L. Ballot, *Z. Phys. A* **302**, 347 (1981).
- [46] V. D. Efros, *Sov. J. Nucl. Phys.* **15**, 128 (1972); **27**, 448 (1979).
- [47] V. F. Demin, *Sov. J. Nucl. Phys.* **26**, 379 (1977).
- [48] M. Fabre de la Ripelle, *Ann. Phys. (NY)* **147**, 281 (1983).
- [49] R. A. Malfliet and J. A. Tjon, *Nucl. Phys.* **A217**, 161 (1969).
- [50] M. S. Kildushov, *Sov. J. Nucl. Phys.* **16**, 117 (1973).
- [51] V. D. Efros, *Sov. J. Nucl. Phys.* **30**, 43 (1979).
- [52] A. Novoselsky and J. Katriel, *Phys. Rev. A* **49**, 833 (1994); *Ann. Phys.* **256**, 192 (1997).
- [53] L. Deng, D. Li, Y. Wang, and C. Deng, *Phys. Rev. A* **51**, 163 (1995).
- [54] V. D. Efros, *Few-Body Systems* **19**, 167 (1995).
- [55] M. Viviani, *Few-Body Systems* **25**, 177 (1998).
- [56] A. Kievsky, L. E. Marcucci, S. Rosati, and M. Viviani, *Few-Body Systems* **22**, 1 (1997).
- [57] F. Zernike and H. C. Brinkman, *Proc. Kon. Ned. Acad. Wensch.* **33**, 3 (1935).
- [58] A. Nogga, H. Kamada, and W. Glöckle, *Few-Body Systems Suppl.* **10**, 41 (1999).
- [59] B. N. Zakharyev, V. V. Pustovalov, and E. D. Efros, *Sov. J. Nucl. Phys.* **8**, 234 (1969).
- [60] T. R. Schneider, *Phys. Lett.* **B40**, 439 (1972).
- [61] M. Viviani, A. Kievsky, and S. Rosati, *Nuovo Cimento* **105 A**, 1473 (1992).
- [62] K. Varga, private communications (please note that the SVM result reported in Ref. [26] in Table V has been probably computed with a different version of the ATTS3 potential).
- [63] Y. Akaishi, *International Review of Nuclear Physics* (World Scientific, Singapore, 1986), Vol. 4, p. 259.
- [64] A. B. Volkov, *Nucl. Phys.* **74**, 33 (1965).
- [65] I. R. Afnan and Y. C. Tang, *Phys. Rev.* **175**, 1337 (1968).
- [66] D. R. Thompson, M. LeMere, and Y. C. Tang, *Nucl. Phys.* **A286**, 53 (1977).
- [67] V. G. J. Stoks, R. A. M. Klomp, M. C. M. Rentmeester, and J. J. deSwart, *Phys. Rev. C* **48**, 792 (1993).
- [68] J. L. Friar, D. Hüber, and U. van Kolck, *Phys. Rev. C* **59**, 53 (1999).
- [69] D. H. Beck and R. D. McKeown, *Ann. Rev. Nucl. Part. Sci.* **51**, 189 (2001) (hep-ph/0102334).
- [70] Jefferson Lab. proposal E00-114, “Parity Violation from ^4He at Low Q^2 : A Clean Measurement of ρ_s ,” accepted by PAC 18, D. S. Armstrong and R. Michaels spokespersons (HAPPEX collaboration) (web page: <http://hallaweb.jlab.org/experiment/HAPPEX/>).
- [71] S. Ramavataram, E. Hadjimichael, and T. W. Donnelly, *Phys. Rev. C* **50**, 1175 (1994).
- [72] E. J. Stephenson *et al.*, *Phys. Rev. Lett.* **91**, 142302 (2003).
- [73] A. Gardestig *et al.*, *Phys. Rev. C* **69**, 044606 (2004).
- [74] N. Barnea *et al.*, *Few-Body Systems* **35**, 155 (2004); see also arXiv:nucl-th/0404086.
- [75] S. A. Tonsfeldt, T. B. Clegg, E. J. Ludwig, Y. Tagishi, and J. F. Wilkerson, *Phys. Rev. Lett.* **45**, 2008 (1980).
- [76] F. D. Santos *et al.*, *Phys. Rev. C* **25**, R3243 (1982).
- [77] B. C. Karp, E. J. Ludwig, W. J. Thompson, and F. D. Santos, *Phys. Rev. Lett.* **53**, 1619 (1984); *Nucl. Phys.* **A457**, 15 (1986).
- [78] H. R. Weller *et al.*, *Phys. Rev. C* **34**, 32 (1986).
- [79] A. Nogga *et al.*, *Phys. Rev. C* **67**, 034004 (2003).
- [80] N. K. Timofeyuk, *Nucl. Phys.* **A632**, 19 (1998), and references therein.
- [81] S. K. Adhikari, T. Frederico, I. D. Goldman, and S. S. Sharma, *Phys. Rev. C* **50**, 822 (1994).
- [82] F. Merz *et al.*, *Phys. Lett.* **B183**, 144 (1987).
- [83] M. Viviani, A. Kievsky, and S. Rosati, in preparation.
- [84] S. Rosati, M. Viviani, and A. Kievsky, *Few-Body Systems Suppl.* **8**, 21 (1995).
- [85] J. Carlson, V. R. Pandharipande, and R. B. Wiringa, *Nucl. Phys.* **A401**, 59 (1983).
- [86] A. Bohr and B. R. Mottelson, *Nuclear Structure* (Benjamin, New York, 1969), Vol. I.